Automatica 100 (2019) 38–51

Contents lists available at ScienceDirect

Automatica

journal homepage: www.elsevier.com/locate/automatica

Traffic congestion control for Aw–Rascle–Zhang model☆

Huan Yu *, Miroslav Krstic

Department of Mechanical and Aerospace Engineering, University of California, San Diego, La Jolla, CA, 92093, United States

ARTICLE INFO

Article history:
Received 7 November 2017
Received in revised form 5 September 2018
Accepted 11 September 2018

Keywords:
ARZ traffic model
PDE control
Backstepping
Adaptive output feedback

ABSTRACT

This paper develops boundary feedback control laws to reduce stop-and-go oscillations in congested traffic. The macroscopic traffic dynamics are governed by Aw–Rascle–Zhang (ARZ) model, consisting of second-order nonlinear partial differential equations (PDEs). A criterion to distinguish free and congested regimes for the ARZ traffic model leads to the study of hetero-directional hyperbolic PDE model of congested traffic regime. To stabilize the oscillations of traffic density and speed in a freeway segment, a boundary input through ramp metering is considered. We discuss the stabilization problem for freeway segments respectively, upstream and downstream of the ramp. For the more challenging upstream control problem, our full-state feedback control law employs a backstepping transformation. Both collocated and anti-collocated boundary observers are designed. The exponential stability in L^2 sense and finite time convergence to equilibrium are achieved and validated with simulation. In the absence of relaxation time and boundary parameters' knowledge, we propose adaptive output feedback control design. Control is applied at outlet and the measurement is taken from inlet of the freeway segment. We use the backstepping method to obtain an observer canonical form in which unknown parameters multiply with measured output. A parametric model based on this form is derived and gradient-based parameter estimators are designed. An explicit state observer involving the delayed values of the input and the output is introduced for state estimation. Using the parameter and state estimates, we develop an adaptive output feedback control law which achieves convergence to the steady regulation in the L^2 sense.

1. Introduction

The stop-and-go traffic is a common phenomenon in congested freeway, causing increase consumptions of fuel and unsafe driving conditions. The oscillations appear with no apparent road change and are caused by delay of a driver's response. It is of great importance if we can reduce this kind of traffic congestion. The traffic instabilities, also known as "jamiton", Belletti, Huo, Litrico, and Bayen (2015), Fan, Herty, and Seibold (0000), Flynn, Kasimov, Nave, Rosales, and Seibold (2009) and Seibold, Flynn, Kasimov, and Rosales (2012) are well represented by Aw–Rascle–Zhang (ARZ) model (Aw & Rascle, 2000; Zhang, 2002), which consists of second-order, nonlinear hyperbolic PDEs of traffic density and velocity.

The traffic congestion on freeway has been investigated intensively with different levels of traffic model. Macroscopic modeling of traffic dynamics with PDE has been proposed, including first-order model by Ligthill and Whitham and Richards (LWR) (Lighthill & Whitham, 1955; Richards, 1956), second-order Payne–Whitham (PW) model (Payne, 1971; Whitham, 2011) and second-order ARZ model. The first-order LWR model fails to model stop-and-go traffic, which does not obey the density–velocity relation in equilibrium. To improve the LWR model, PW model developed a velocity equation to allow deviations from the density–velocity equilibrium. The PW model, consisting of the momentum equation and conservation law, is nonlinear second-order PDEs. It is shown in Cassidy and Windover (1995) and Daganzo (1995) that disturbances in PW model travel faster than traffic velocity. As a result, vehicle on freeway is influenced from both behind and front, indicating that traffic flow is isotropic. However, Zhang (2002) pointed out that traffic flow is anisotropic since drivers mostly respond to the traffic in front of them. To deal with this, Aw and Rascle (2000) and Zhang (2002) separately proposed a new velocity equation to deal with the problem. Combining these two models together by proper definition and choice of coefficients, the ARZ model is used in this paper.

To stabilize the oscillations of stop-and-go traffic, we propose boundary control strategies. Boundary control through ramp metering and varying speed limits are widely and effectively used nowadays in freeway traffic management. In developing boundary feedback control through ramp metering and varying speed limits, many recent efforts (Belletti et al., 2015; Karafyllis, Bekiaris-Liberis,

☆ Huan Yu acknowledges financial support of China Scholarship Council (CSC). The material in this paper was partially presented at the 2018 American Control Conference, June 27–29, Milwaukee, WI, USA. This paper was recommended for publication in revised form by Associate Editor Thomas Meurer under the direction of Editor Daniel Liberzon.

* Corresponding author.
E-mail addresses: huy015@eng.ucsd.edu (H. Yu), krstic@ucsd.edu (M. Krstic).

https://doi.org/10.1016/j.automatica.2018.10.040
0005-1098/

& Papageorgiou, 2017; Zhang & Prieur, 2017) focus on ARZ model, due to its simplicity and realism. In Belletti et al. (2015), spectral analysis is applied to the linearized ARZ model and a parameter comparable to Froude number is proposed to classify different regimes in traffic flow. The boundary control and measurement are designed based on the spectral analysis. Zhang and Prieur (2017) investigate the local stability of a positive hyperbolic system with application to the ARZ model and Karafyllis et al. (2017) provide a boundary control law that achieves global stabilization. The control strategy developed in Belletti et al. (2015) and Zhang and Prieur (2017) both needed coordination of ramp metering and varying speed limits. The previously cited results Zhang & Prieur (2017) and Karafyllis et al. (2017) considered the homogeneous ARZ model, neglecting the relaxation term which reflects adaptation of driver's behavior to traffic conditions (Fan, Herty, & Seibold, 2013). In this paper, the relaxation term is kept in the ARZ model and therefore the inhomogeneous ARZ model is considered which preserves more potential to yield a realistic prediction. More importantly, only the inhomogeneous ARZ model considering the delay of driver's response is able to describe the instabilities of uniform states in stop-and-go traffic problem. At the same time, only ramp metering control is implemented which is more applicable in practice. Furthermore, the adaptive control problem is solved. The stabilization of ARZ model is achieved without knowing some boundary parameters and relaxation time.

The key idea of our control design is applying backstepping method to ARZ model which is a hyperbolic PDE system. Theoretical results on boundary control design for PDEs using backstepping method have been developed for 2×2 coupled hyperbolic systems in Anfinsen and Aamo (2018), Coron, Vazquez, Krstic, and Bastin (2013), Deutscher (2017a, b), Vazquez, Krstic, and Coron (2011), and Yu, Vazquez, and Krstic (2017), and general heterodirectional hyperbolic systems in Anfinsen, Diagne, Aamo, and Krstic (2016), Auriol and Meglio (2016), Deutscher (2017c), Hasan, Aamo, and Krstic (2016), Hu, Meglio, Vazquez, and Krstic (2016), Meglio, Argomedo, Hu, and Krstic (2016), Meglio, Vazquez, and Krstic (2013), and Su, Wang, and Krstic (2017). We adopt and enhance the existing methodology to fit the ARZ model. This is an essential step for boundary control of freeway traffic in its PDE formulation. We develop full-state feedback boundary control law, boundary observer based on Vazquez et al. (2011) and further enhanced the adaptive control design based on Yu et al. (2017). We address the problem of unknown parameter coupling with boundary measurement which is absent in the previous literature.

The main contribution of this paper: this is the first result on boundary feedback control of inhomogeneous ARZ model to authors knowledge. We address the traffic dynamics with ARZ PDE model from control perspectives, explore the general framework for stabilization problem of stop-and-go traffic and develop boundary feedback control design including both nonadaptive and adaptive designs. Motivated by the ARZ PDE model, our work yields some theoretical advance relative to previous results on adaptive control design for hyperbolic systems. Most importantly, this result paves the way for addressing the traffic problem with PDE boundary control, as one of its most important application.

The outline is as follows: Section 2 presents linearized ARZ model and free/congested regime. Section 3 proposes a general freeway traffic control model through ramp-metering. Sections 4 and 5 provide boundary control design for downstream of the ramp metering traffic and full-state feedback control law and observers for upstream of the ramp metering traffic. Section 6 gives adaptive output feedback design for the upstream of ramp metering problem. Both the nonadaptive control design and adaptive design are validated with simulation in Section 7. Section 8 summarizes results and discusses future work of this paper.

2. Problem statement

We consider the Aw–Rascle–Zhang model with a relaxation term and linearize it around steady states.

2.1. Aw–Rascle–Zhang model

The Aw–Rascle model is

$$\partial_t \rho + \partial_x(\rho v) = 0, \tag{1}$$

$$\partial_t v + (v - \rho p'(\rho))\partial_x v = \frac{V(\rho) - v}{\tau}. \tag{2}$$

The state variable $\rho(x,t)$ is the traffic density and $v(x,t)$ is the traffic speed, $V(\rho)$ is the equilibrium traffic speed profile and τ is the relaxation time related to driving behavior. The variable $p(\rho)$ is defined as the traffic pressure, an increasing function of density

$$p(\rho) = \rho^\gamma, \tag{3}$$

and $\gamma \in \mathbb{R}_+$.

The Zhang model is given by

$$\partial_t \rho + \partial_x(\rho v) = 0, \tag{4}$$

$$\partial_t v + \left(v + \rho V'(\rho)\right)\partial_x v = 0. \tag{5}$$

Combining these two models together, we have the Aw–Rascle–Zhang model in (ρ, v) given in (1), (2), and the conditions $p'(\rho) = -V'(\rho)$ and $p(0) = 0$ need to be satisfied so that the Aw–Rascle model and the Zhang model are consistent. Thus it holds that

$$p(\rho) = v_f - V(\rho), \tag{6}$$

where v_f is the free flow velocity. Since $V(\rho_m) = 0$ and ρ_m is the maximum density, $p(\rho) = \rho^\gamma$ is rescaled as

$$p(\rho) = v_f \left(\frac{\rho}{\rho_m}\right)^\gamma. \tag{7}$$

The equilibrium velocity–density relationship $V(\rho)$ is given in the form of Greenshield's model (Greenshields, Bibbins, Channing, & Miller, 1935),

$$V(\rho) = v_f - p(\rho) = v_f \left(1 - \left(\frac{\rho}{\rho_m}\right)^\gamma\right). \tag{8}$$

2.2. Linearized ARZ model

The traffic density is the number of vehicles per unit length. The traffic flux is defined as the number of vehicles per unit time which cross a given point on the road, which is a more reasonable physical variable to control by ramp metering. Therefore, we rewrite the ARZ model in traffic flux and velocity (q, v),

$$q_t + v q_x = \frac{q(\gamma p - v)}{v} v_x + \frac{q(v_f - p - v)}{\tau v}, \tag{9}$$

$$v_t - (\gamma p - v) v_x = \frac{v_f - p - v}{\tau}, \tag{10}$$

where the traffic flow flux q is defined as

$$q = \rho v. \tag{11}$$

The traffic pressure $p(\rho)$ and flux q are related by

$$p = \frac{v_f}{\rho_m^\gamma} \left(\frac{q}{v}\right)^\gamma. \tag{12}$$

There is no explicit solution to the nonlinear hyperbolic (q, v)-system in (9), (10). To better understand the dynamics of the ARZ

traffic model, we linearize the model around steady states $(q^\star, v^\star)$. The small deviations from the nominal profile are defined as

$$\tilde{q}(x,t) = q(x,t) - q^\star, \tag{13}$$
$$\tilde{v}(x,t) = v(x,t) - v^\star, \tag{14}$$

where $x \in [0, L]$, $t \in [0, \infty)$.

We consider the traffic dynamics of a segment of freeway and L is the length of freeway segment. For inlet boundary at $x = 0$, we consider a constant traffic flux $q^\star$ entering the domain which can be realized by implementing a mainline flux metering at the inlet,

$$q(0,t) = q^\star. \tag{15}$$

For outlet, we assume to implement a mainline density metering so that the following condition holds,

$$\rho(L,t) = \rho^\star. \tag{16}$$

Applying this assumption to the outlet boundary $x = L$ of considered freeway section and we obtain a boundary condition for (q, v)-system in (9), (10),

$$v(L,t) = \frac{1}{\rho^\star} q(L,t). \tag{17}$$

The linearized ARZ model is described with the following $(\tilde{q}, \tilde{v})$-system,

$$\tilde{q}_t + v^\star \tilde{q}_x - \frac{q^\star(\gamma p^\star - v^\star)}{v^\star}\tilde{v}_x = -\frac{q^\star}{\tau}\left(\frac{1}{v^\star} - \frac{1}{\gamma p^\star}\right)\tilde{v} - \frac{\gamma p^\star}{\tau v^\star}\tilde{q}, \tag{18}$$

$$\tilde{v}_t - (\gamma p^\star - v^\star)\tilde{v}_x = \frac{\gamma p^\star - v^\star}{\tau v^\star}\tilde{v} - \frac{\gamma p^\star}{\tau q^\star}\tilde{q}, \tag{19}$$

with the linearized boundary conditions

$$\tilde{q}(0,t) = 0, \tag{20}$$
$$\tilde{v}(L,t) = \frac{1}{\rho^\star}\tilde{q}(L,t). \tag{21}$$

where $p^\star = p(q^\star, v^\star)$, according to (12).

2.3. Free/congested regime analysis

According to the relation between $p^\star$ and $v^\star$ in (6), the following holds

$$v^\star - \gamma p^\star = v^\star - \gamma(v_f - v^\star) = (1+\gamma)v^\star - \gamma v_f. \tag{22}$$

For free-flow regime, $\gamma p^\star < v^\star$ implies $v^\star > \frac{\gamma}{\gamma+1} v_f$. For congested regime, $\gamma p^\star > v^\star$ implies $v^\star < \frac{\gamma}{\gamma+1} v_f$. Therefore, $v^\star = \frac{\gamma}{\gamma+1} v_f$ is the critical velocity to distinguish the free regime and the congested regime of traffic flow.

- Free-flow regime : $\rho^\star < \frac{\rho_m}{(1+\gamma)^{1/\gamma}} \Leftrightarrow v^\star > \frac{\gamma}{\gamma+1} v_f$.
  In the free-flow regime, both the disturbances of traffic flux and velocity travel downstream, at respective speeds $v^\star$ and $v^\star - \gamma p^\star$. The linearized ARZ model in free-regime is a homo-directional hyperbolic PDEs.
- Congested regime : $\rho^\star > \frac{\rho_m}{(1+\gamma)^{1/\gamma}} \Leftrightarrow v^\star < \frac{\gamma}{\gamma+1} v_f$.
  In the congested regime, the disturbances of the traffic flow flux are carried downstream by the vehicles that generated them. The disturbances of the traffic speed travel upstream at a speed of $\gamma p^\star - v^\star$. Therefore, we are dealing with a hetero-directional coupled hyperbolic system, given that $v^\star - \gamma p^\star < 0$ and $v^\star > 0$ in the congested regime. The disturbances force vehicles into deceleration–acceleration cycles, leading to the traffic oscillations, known as the stop-and-go traffic. This kind of instability in traffic causes unsafe driving conditions, extra fuel consumptions and eventually evolves into a bumper-to-bumper jam.
- Bumper-to-bumper traffic jam : $\rho^\star = \rho_m \Leftrightarrow v^\star = 0$
  The traffic becomes bumper-to-bumper jammed when the traffic density reaches its maximum and traffic speed equals 0.

In this paper, we focus on control design for the congested regime

$$\rho_m > \rho^\star > \frac{\rho_m}{(1+\gamma)^{1/\gamma}} \Leftrightarrow 0 < v^\star < \frac{\gamma}{1+\gamma} v_f. \tag{23}$$

We choose the steady states $(\rho^\star, v^\star)$ satisfying above inequalities but not too close to bounds so that small disturbances will not exceed them.

3. Boundary control model

Before we apply boundary control to the linearized ARZ model in $(\tilde{q}, \tilde{v})$, we represent the system in Riemann coordinates and then map it to a decoupled first-order 2×2 hyperbolic system in $(\bar{w}, \bar{v})$. We propose two different control strategies for the hyperbolic $(\bar{w}, \bar{v})$-system through ramp metering control.

3.1. Mapping to a first-order 2×2 hyperbolic system

We define new variables $(w, \bar{v})$ in Riemann coordinates,

$$w = \tilde{q} - q^\star\left(\frac{1}{v^\star} - \frac{1}{\gamma p^\star}\right)\tilde{v}, \tag{24}$$

$$\bar{v} = \frac{q^\star}{\gamma p^\star}\tilde{v}, \tag{25}$$

We obtain

$$w_t(x,t) + v^\star w_x(x,t) = -\frac{1}{\tau} w, \tag{26}$$
$$\bar{v}_t(x,t) - (\gamma p^\star - v^\star)\bar{v}_x(x,t) = -\frac{1}{\tau} w, \tag{27}$$
$$w(0,t) = -\frac{\gamma p^\star - v^\star}{v^\star}\bar{v}(0,t), \tag{28}$$
$$\bar{v}(L,t) = w(L,t). \tag{29}$$

In order to decouple (26) and (29), we introduce a scaled state as follows:

$$\bar{w}(x,t) = \exp\left(\frac{x}{\tau v^\star}\right) w(x,t). \tag{30}$$

The $(w, \bar{v})$-system is then transformed to a first-order 2×2 hyperbolic system

$$\bar{w}_t(x,t) = -v^\star \bar{w}_x(x,t), \tag{31}$$
$$\bar{v}_t(x,t) = (\gamma p^\star - v^\star)\bar{v}_x(x,t) + c(x)\bar{w}(x,t), \tag{32}$$
$$\bar{w}(0,t) = -k_0 \bar{v}(0,t), \tag{33}$$
$$\bar{v}(L,t) = \kappa \bar{w}(L,t). \tag{34}$$

where

$$c(x) = -\frac{1}{\tau}\exp\left(-\frac{x}{\tau v^\star}\right), \tag{35}$$
$$k_0 = \frac{\gamma p^\star - v^\star}{v^\star}, \tag{36}$$
$$\kappa = \exp\left(\frac{-L}{\tau v^\star}\right). \tag{37}$$

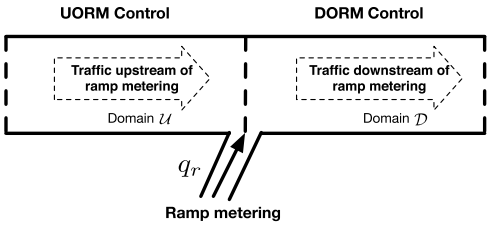

Fig. 1. A freeway segment controlled by ramp-metering.

The spatially varying coefficient $c(x)$ is a strictly increasing function and is bounded by

$$-\frac{1}{\tau} \leq c(x) \leq -\frac{\kappa}{\tau}. \tag{38}$$

The following relations for boundary values are obtained from (24)–(25),

$$\tilde{q}(0,t) = \bar{w}(0,t) + k_0 \bar{v}(0,t), \tag{39}$$
$$\tilde{q}(L,t) = \kappa \bar{w}(L,t) + k_0 \bar{v}(L,t), \tag{40}$$

The applicable boundary control inputs could be traffic flow flux at either the inlet or at the outlet of a freeway section. We summarize the transformation from the linearized Aw–Rascle–Zhang model in $(\tilde{q}, \tilde{v})$-system to $(\bar{w}, \bar{v})$-system,

$$\bar{w}(x,t) = \exp\left(\frac{x}{\tau v^\star}\right)\left(\tilde{q}(x,t) - \rho_1 \tilde{v}(x,t)\right), \tag{41}$$
$$\bar{v}(x,t) = \rho_2 \tilde{v}(\xi,t). \tag{42}$$

And the inverse transformation is given by

$$\tilde{q}(x,t) = \exp\left(-\frac{x}{\tau v^\star}\right)\bar{w}(x,t) + k_0 \bar{v}(x,t), \tag{43}$$
$$\tilde{v}(x,t) = \frac{1}{\rho_2}\bar{v}(\xi,t). \tag{44}$$

where the constant, positive coefficients are defined as follows:

$$\rho_1 = q^\star\left(\frac{1}{v^\star} - \frac{1}{\gamma p^\star}\right), \quad \rho_2 = \frac{q^\star}{\gamma p^\star}. \tag{45}$$

Therefore, we can study the stability of $(\tilde{q}, \tilde{v})$-system through $(\bar{w}, \bar{v})$-system due to their equivalence. The control laws we obtain later for the $(\bar{w}, \bar{v})$-system guarantee the equivalent stability properties of the $(\tilde{q}, \tilde{v})$-system.

3.2. UORM/DORM ramp metering control

Considering a ramp metering is installed at freeway on-ramp to reduce the oscillations in the congested traffic, we propose two different control designs based on the domain we aim to control with the ramp metering. (See Fig. 1.)

If we consider controlling the traffic downstream of the ramp metering (DORM) in the domain $\mathscr{D}$, the ramp metering is located at the inlet of the domain $\mathscr{D}$ and $U_{\text{in}}(t)$ is the control law to be designed. The DORM controller $U_{\text{in}}(t)$ is applied with $\tilde{q}(0,t)$.

In the case that we control the traffic upstream of the ramp metering (UORM) in the domain $\mathscr{U}$, the controller $U_{\text{out}}(t)$ is located at the outlet of domain $\mathscr{U}$. The UORM controller $U_{\text{out}}(t)$ is applied with $\tilde{q}(L,t)$.

3.2.1. DORM control

We define a ramp metering boundary control input $U_{\text{in}}(t)$ at the inlet of $\mathscr{D}$,

$$U_{\text{in}}(t) = q_r(t) = \tilde{q}(0,t), \tag{46}$$
$$\tilde{q}(L,t) = \rho^\star \tilde{v}(L,t). \tag{47}$$

Note that the DORM controller $U_{\text{in}}(t)$ is applied with the traffic flow flux variation at the inlet of domain $\mathscr{D}$. The other boundary condition does not change. We need to implement a density metering at mainline outlet so that a constant density is enforced.

Substituting (46) into (39), we obtain the controlled boundary. The DORM control model is given by $(\bar{w}, \bar{v})$-system in (31), (32) with controlled boundary at the inlet in (50),

$$\bar{w}_t(x,t) = -v^\star \bar{w}_x(x,t), \tag{48}$$
$$\bar{v}_t(x,t) = (\gamma p^\star - v^\star)\bar{v}_x(x,t) + c(x)\bar{w}(x,t), \tag{49}$$
$$\bar{w}(0,t) = -k_0 \bar{v}(0,t) + U_{\text{in}}(t), \tag{50}$$
$$\bar{v}(L,t) = \kappa \bar{w}(L,t). \tag{51}$$

3.2.2. UORM control

We consider a constant traffic flux entering the domain $\mathscr{U}$ and the control input $U_{\text{out}}(t)$ is implemented with the ramp metering at the outlet of the domain. For inlet, we need to implement a flux metering at mainline so that a constant flux is enforced. The UORM control input $U_{\text{out}}(t)$ and $\tilde{q}(0,t)$ are defined as

$$U_{\text{out}}(t) = q_r(t), \tag{52}$$
$$\tilde{q}(0,t) = 0. \tag{53}$$

The total traffic flow flux variation at the outlet of domain $\mathscr{U}$ includes the traffic flow flux variation from the mainline and from the ramp.

$$\tilde{q}(L^+,t) = \tilde{q}(L^-,t) + q_r(t). \tag{54}$$

The mainline flow flux variation $\tilde{q}(L^-,t)$ in the domain is given by (40). The flow flux variation $\tilde{q}(L^+,t)$ of the downstream of domain $\mathscr{U}$ is given by (21). Substituting (40) and (21) into (54), we obtain the UORM control model with controlled boundary at the outlet in (58).

$$\bar{w}_t(x,t) = -v^\star \bar{w}_x(x,t), \tag{55}$$
$$\bar{v}_t(x,t) = (\gamma p^\star - v^\star)\bar{v}_x(x,t) + c(x)\bar{w}(x,t), \tag{56}$$
$$\bar{w}(0,t) = -k_0 \bar{v}(0,t), \tag{57}$$
$$\bar{v}(L,t) = \kappa \bar{w}(L,t) + U_{\text{out}}(t), \tag{58}$$

3.3. Spectrum analysis of control models with zero input

In order to explore the traffic dynamics in the open loop-system, we consider the zero input for DORM or UORM control design

$$q_r(t) = 0, \tag{59}$$
$$U_{\text{in}}(t) = 0, \quad U_{\text{out}}(t) = 0. \tag{60}$$

According to boundary conditions in (50), (51) or (57), (58), we have the following zero input system that holds for both control models

$$\bar{w}_t(x,t) = -v^\star \bar{w}_x(x,t), \tag{61}$$
$$\bar{v}_t(x,t) = (\gamma p^\star - v^\star)\bar{v}_x(x,t) + c(x)\bar{w}(x,t), \tag{62}$$
$$\bar{w}(0,t) = -k_0 \bar{v}(0,t), \tag{63}$$
$$\bar{v}(L,t) = \kappa \bar{w}(L,t), \tag{64}$$

where $x \in [0, L]$ and $t > 0$. The diagram is shown in Fig. 2.

The above zero-input system is equivalent to the open-loop $(\tilde{q}, \tilde{v})$-system in (18)–(21).

In order to analyze the spectrum of the system with zero input in (61)–(64), we transform the first-order 2×2 hyperbolic system to a second-order wave equation.

$$y_{tt}(x,t) = v^\star(\gamma p^\star - v^\star)y_{xx}(x,t) - (2v^\star - \gamma p^\star)y_{xt}(x,t) - \frac{1}{\tau}y_t(x,t) + \frac{\gamma p^\star - v^\star}{\tau}y_x(x,t), \tag{65}$$
$$y_t(0,t) = 0, \tag{66}$$
$$y_x(L,t) = 0. \tag{67}$$

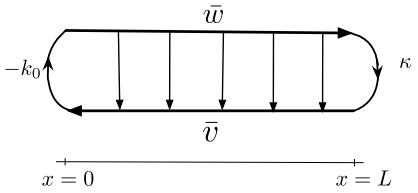

Fig. 2. Diagram of control model with zero input.

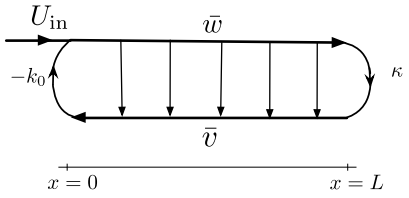

Fig. 3. Time response of DORM control model.

The new variable $y(x,t)$ satisfies the following relations,

$$\begin{aligned} w(x,t) =& y_t(x,t) - (\gamma p^\star - v^\star) y_x(x,t), \\ \bar{v}(x,t) =& y_t(x,t) + v^\star y_x(x,t). \end{aligned} \tag{68}$$

The term y_{xt} is a structural damping, of which effect is fully addressed in D'Abbicco and Reissig (2014). The term y_t is also a damping term and the longer reaction time τ will cause the weaker damping effect of y_t in the domain.

The wave equation is written in the vector form,

$$\frac{\partial}{\partial t}\begin{pmatrix} y \\ y_t \end{pmatrix} = A \begin{pmatrix} y \\ y_t \end{pmatrix}, \tag{69}$$

where the operator matrix A is

$$\begin{pmatrix} y_t \\ -\frac{1}{\tau} y_t - (2v^\star - \gamma p^\star) y_{xt} + \frac{\gamma p^\star - v^\star}{\tau} y_x + v^\star(\gamma p^\star - v^\star) y_{xx} \end{pmatrix}.$$

The eigenvalues of A are obtained by solving the following equations,

$$\lambda y = y_t, \tag{70}$$

$$\begin{aligned} \lambda^2 y =& -(2v^\star - \gamma p^\star)\lambda y_x - \frac{\lambda}{\tau} \\ &+ \frac{\gamma p^\star - v^\star}{\tau} y_x + v^\star(\gamma p^\star - v^\star) y_{xx}. \end{aligned} \tag{71}$$

We take Fourier transform with respect to the spatial variable $x \in [0, L]$. We map $y(x,t) \to \hat{y}(n,t)$, $n \in \mathbb{Z}$,

$$y(x) = \sum_{n=1}^{\infty} \hat{y}_n \exp\left(\frac{inx}{L}\right). \tag{72}$$

The nth Fourier coefficient is defined as

$$\hat{y}_n = \int_0^L y(x) \exp\left(\frac{-inx}{L}\right) dx, \tag{73}$$

the transformation yields

$$\hat{y}_x = \frac{inx}{L}\hat{y}, \quad \hat{y}_{xx} = \frac{-n^2}{L^2}\hat{y}. \tag{74}$$

Substituting $\hat{y}_x$ and $\hat{y}_{xx}$ into (71), the kth pair of eigenvalues satisfies the following quadratic equation:

$$\begin{aligned} 0 =& \lambda^2 + \left(\frac{2v^\star - \gamma p^\star}{L} ni + \frac{1}{\tau}\right)\lambda \\ &+ \frac{v^\star(\gamma p^\star - v^\star)}{L^2} n^2 - \frac{\gamma p^\star - v^\star}{\tau L} ni. \end{aligned} \tag{75}$$

The nth pair of eigenvalues is obtained by solving the quadratic equation,

$$\lambda_{1,2} = \frac{-\frac{1}{\tau} - \frac{(2v^\star - \gamma p^\star)}{L} ni \pm (\frac{1}{\tau} + \frac{\gamma p^\star}{L} ni)}{2}. \tag{76}$$

Thus there are two sets of eigenvalues in the left half plane,

$$\lambda_1 = \frac{\gamma p^\star - v^\star}{L} ni, \quad \lambda_2 = -\frac{1}{\tau} - \frac{v^\star}{L} ni. \tag{77}$$

The eigenvalue λ_1 only contains the imaginary part. The longer the relaxation time τ, the smaller the negative real part in the eigenvalue λ_2. As $\tau \to \infty$ and $n \to \infty$,

$$\lambda_1 \to \text{Im}(+\infty), \quad \lambda_2 \to \text{Im}(-\infty). \tag{78}$$

According to the above spectral analysis, two sets of eigenvalues locate along the imaginary axis. The system is marginal stable and there are persistent oscillations in the domain of the zero input system in (61)–(64). Therefore, it is meaningful to propose control design for the system.

4. DORM control design

The DORM control problem is given by

$$\bar{w}_t(x,t) = -v^\star \bar{w}_x(x,t), \tag{79}$$

$$\bar{v}_t(x,t) = (\gamma p^\star - v^\star)\bar{v}_x(x,t) + c(x)\bar{w}(x,t), \tag{80}$$

$$\bar{w}(0,t) = -k_0 \bar{v}(0,t) + U_{\text{in}}(t), \tag{81}$$

$$\bar{v}(L,t) = \kappa \bar{w}(L,t), \tag{82}$$

where $x \in \mathscr{D} \triangleq [0, L]$ and $t > 0$. The diagram of DORM control model is shown in Fig. 3.

If we choose the DORM controller as

$$U_{\text{in}}(t) = k_0 \bar{v}(0,t), \tag{83}$$

we get $\bar{w}(0,t) = 0$. The explicit solution to the above $(\bar{w}, \bar{v})$-system with the DORM control law (83) is

$$\bar{w}(x,t) = \begin{cases} \bar{w}(x - v^\star t, 0), & t < \dfrac{x}{v^\star}, \\ \bar{w}\left(0, t - \dfrac{x}{v^\star}\right), & t \geq \dfrac{x}{v^\star}, \end{cases} \tag{84}$$

and for $t \geq \frac{x}{v^\star}$,

$$\bar{w}(x,t) \equiv 0. \tag{85}$$

Solving for $\bar{v}(x,t)$, we have

$$\bar{v}(x,t) = \begin{cases} \bar{v}(x + (\gamma p^\star - v^\star)t, 0) \\ + \displaystyle\int_0^t c(x + (\gamma p^\star - v^\star)(t-s))\bar{w}(0,s)ds, \\ \qquad\qquad t < \dfrac{L-x}{\gamma p^\star - v^\star}, \\ \kappa \bar{w}\left(L, t - \dfrac{L-x}{\gamma p^\star - v^\star}\right) \\ + \dfrac{1}{\gamma p^\star - v^\star} \displaystyle\int_x^L c(s)\bar{w}\left(0, t + \dfrac{x-s}{\gamma p^\star - v^\star}\right) ds, \\ \qquad\qquad t \geq \dfrac{L-x}{\gamma p^\star - v^\star}. \end{cases} \tag{86}$$

Thus for $t \geq t_f$, it holds that

$$\bar{v}(x,t) \equiv 0. \tag{87}$$

where

$$t_f = \frac{L}{v^\star} + \frac{L}{\gamma p^\star - v^\star}. \tag{88}$$

Substituting k_0 in (36) and $\bar{v}$ in (42), we get

$$U_{\text{in}}(t) = \rho_1 \tilde{v}(0,t). \tag{89}$$

The DORM boundary controller $U_{\text{in}}(t)$ is obtained by the measurement of $\tilde{v}(0,t)$. To show the exponential stability of the system in the L^2 sense, we construct the following Lyapunov functions

$$V_1(t) = \frac{1}{2v^\star}\int_0^L e^{-x}\bar{w}^2(x,t)dx, \tag{90}$$

$$V_2(t) = \frac{1}{2(\gamma p^\star - v^\star)}\int_0^L e^{x}\bar{v}^2(x,t)dx, \tag{91}$$

and differentiate the Lyapunov functions in time. We obtain the following inequalities using Cauchy–Schwarz Inequality and Young's Inequality,

$$\dot{V}_1 \le -e^{-L}(\bar{w}^2(L) + \|\bar{w}\|^2), \tag{92}$$

$$\begin{aligned}\dot{V}_2 \le& e^{L}\bar{v}^2(L) - \bar{v}^2(0) - \|\bar{v}\|^2 \\ &+ \frac{1}{\gamma p^\star - v^\star}\int_0^L e^{x}\bar{v}(x)c(x)\bar{w}(x)dx.\end{aligned} \tag{93}$$

According to the boundedness of $c(x)$ in (38), we have

$$|c(x)| \le C_0 = \frac{1}{\tau} \tag{94}$$

Then it holds that

$$\begin{aligned}\dot{V}_2 \le& e^{L}\kappa^2\bar{w}^2(L) + \frac{1}{2d_1(\gamma p^\star - v^\star)}\|\bar{w}\|^2 \\ &- \left(1 - \frac{d_1 C_0^2 e^{2L}}{2(\gamma p^\star - v^\star)}\right)\|\bar{v}\|^2,\end{aligned} \tag{95}$$

where d_1 is a positive constant and we choose $d_1 < \frac{2\tau^2(\gamma p^\star - v^\star)}{e^{2L}}$. Consider the following Lyapunov function

$$V = d_2 V_1 + V_2, \tag{96}$$

where $d_2 = \max\left(e^{2L}\kappa^2, \frac{e^{2L}}{2d_1(\gamma p^\star - v^\star)}\right)$, it holds that

$$\dot{V} \le -d_0 V, \tag{97}$$

where $d_0 = \min\left(\frac{d_2}{e^L} - \frac{1}{2d_1(\gamma p^\star - v^\star)}, 1 - \frac{d_1 C_0^2 e^{2L}}{2(\gamma p^\star - v^\star)}\right)$. The exponential stability of the system (79)–(82) with the DORM boundary controller (83) is shown above. From the explicit solution of the system, it holds for $t \ge t_f$,

$$\bar{w}(x,t) \equiv 0, \quad \bar{v}(x,t) \equiv 0. \tag{98}$$

We summarize above result in the following Theorem.

Theorem 1. *Consider system (79)–(82) with inital conditions $\bar{w}_0, \bar{v}_0 \in L^2[0,L]$ and the control law (83). The equilibrium $\bar{w} \equiv \bar{v} \equiv 0$ is exponentially stable in the L^2 sense and the equilibrium is reached in finite time $t = t_f$ given in (88).*

5. UORM control designs

For UORM control design, we have

$$\bar{w}_t(x,t) = -v^\star \bar{w}_x(x,t), \tag{99}$$

$$\bar{v}_t(x,t) = (\gamma p^\star - v^\star)\bar{v}_x(x,t) + c(x)\bar{w}(x,t), \tag{100}$$

$$\bar{w}(0,t) = -k_0\bar{v}(0,t), \tag{101}$$

$$\bar{v}(L,t) = \kappa\bar{w}(L,t) + U_{\text{out}}(t), \tag{102}$$

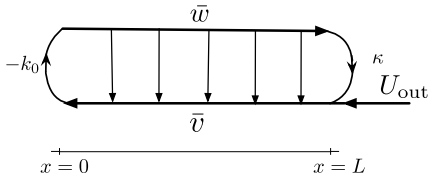

Fig. 4. Time response of UORM control model.

where $x \in \mathscr{U} \triangleq [0, L]$ and $t > 0$. The diagram of the UORM control model is shown in Fig. 4.

5.1. UORM full-state feedback control design

Using the following backstepping transformation, we transform the system of UORM control design (99)–(102) into the target system,

$$\alpha(x,t) = \bar{w}(x,t), \tag{103}$$

$$\begin{aligned}\beta(x,t) =& \bar{v}(x,t) - \int_0^x M(x-\xi)\bar{v}(\xi,t)d\xi \\ &- \int_0^x K(x,\xi)\bar{w}(\xi,t)d\xi.\end{aligned} \tag{104}$$

For boundary conditions, we have $\bar{w}(0,t) = \alpha(0,t)$ and $\bar{v}(0,t) = \beta(0,t)$. The target system is given by

$$\alpha_t(x,t) = -v^\star\alpha_x(x,t), \tag{105}$$

$$\beta_t(x,t) = (\gamma p^\star - v^\star)\beta_x(x,t), \tag{106}$$

$$\alpha(0,t) = -k_0\beta(0,t), \tag{107}$$

$$\beta(L,t) = 0. \tag{108}$$

To obtain the target system, we take time derivative and spatial derivative on (104). The following kernel equations and boundary condition need to be satisfied,

$$(\gamma p^\star - v^\star)K_x - v^\star K_\xi = c(\xi)K(x-\xi,0), \tag{109}$$

$$K(x,x) = -\frac{c(x)}{\gamma p^\star}, \tag{110}$$

where $K(x,\xi)$ evolves in the triangular domain $\mathscr{T} = \{(x,\xi) : 0 \le \xi \le x \le L\}$ and $M(x)$ is defined as

$$M(x) = -K(x,0). \tag{111}$$

The well-posedness of the kernel equations (109)–(111) and the boundedness of kernel variables are obtained following the same steps of the proof in the Appendix of Vazquez et al. (2011). Therefore, invertibility of the backstepping transformation in (103), (104) is established and we can study the target system for stability of the plant.

The UORM full-state feedback controller is chosen as

$$\begin{aligned}U_{\text{out}}(t) =& -\kappa\bar{w}(L,t) + \int_0^L M(L-\xi)\bar{v}(\xi,t)d\xi \\ &+ \int_0^L K(L,\xi)\bar{w}(\xi,t)d\xi,\end{aligned} \tag{112}$$

so that $\beta(L,t) = 0$ is satisfied. One can easily find the explicit solution to the target system (105)–(108) and obtain that

$$\alpha(x,t) \equiv \beta(x,t) \equiv 0, \tag{113}$$

after $t_f = t_\alpha + t_\beta = \frac{L}{v^\star} + \frac{L}{\gamma p^\star - v^\star}$. Thus α and β go to zeros in finite time $t = t_f$. It is straightforward to prove that the α, β system is L^2 exponentially stable. Due to the invertibility of the transformation, $(\bar{w}, \bar{v})$-system is also L^2 exponentially stable.

Theorem 2. *Consider system (99)–(102) with inital conditions $\bar{w}_0$, $\bar{v}_0 \in L^2[0, L]$ and the control law (112) where the kernels $K(x, \xi)$ and $M(x)$ are obtained by solving (109)–(111). The equilibrium $\bar{w} \equiv \bar{v} \equiv 0$ is exponentially stable in the L^2 sense and the equilibrium is reached in finite time $t = t_f$ given in (88).*

Transforming $\bar{w}$ and $\bar{v}$ in (112) to $\tilde{q}$ and $\tilde{v}$ using the inverse transformation in (43)–(44), we get the control law in $(\tilde{q}, \tilde{v})$ as

$$\begin{aligned} U_{\text{out}}(t) =& -\tilde{q}(L, t) + \rho_1 \tilde{v}(L, t) + \rho_1 \int_0^L M(L-\xi)\tilde{v}(\xi, t)d\xi \\ & - \kappa \int_0^L K(L, \xi) \exp\left(\frac{\xi}{\tau v^\star}\right) \tilde{v}(\xi, t)d\xi \\ & + k_0 \int_0^L K(L, \xi) \exp\left(\frac{\xi}{\tau v^\star}\right) \tilde{q}(\xi, t)d\xi. \end{aligned} \tag{114}$$

Due to the invertibility of transformation (41)–(44) between $(\bar{w}, \bar{v})$ and $(\tilde{q}, \tilde{v})$, the $(\tilde{q}, \tilde{v})$-system is exponentially stable and converges to zero in the finite time. Therefore, the (q, v) system is exponentially stable and converges to $(q^\star, v^\star)$ in the finite time t_f.

To obtain $U_{\text{out}}(t)$, we need to take measurement of $\tilde{v}$ and $\tilde{q}$ in the domain $\mathscr{U}$, which might be realized by traffic camera and fleet GPS data. However, we propose the boundary observer design, considering the difficulties and costs to implement sensors along the freeway. We introduce two boundary observers; one is located at the same boundary with the full-state feedback controller and the other one is anti-collocated with the controller.

5.2. UORM anti-collocated boundary observer design

We define the following anti-collocated boundary measurement

$$Y_a(t) = \bar{v}(0, t). \tag{115}$$

According to (42), we obtain $\bar{v}(0, t) = \rho_2 \tilde{v}(0, t)$, by the measurement of $\tilde{v}(0, t)$. Then we design an observer by constructing the following system,

$$\hat{w}_t(x, t) = -v^\star \hat{w}_x(x, t), \tag{116}$$
$$\hat{v}_t(x, t) = (\gamma p^\star - v^\star)\hat{v}_x(x, t) + c(x)\hat{w}(x, t), \tag{117}$$
$$\hat{w}(0, t) = -k_0 Y_a(t), \tag{118}$$
$$\hat{v}(L, t) = \kappa \hat{w}(L, t) + U_{\text{out}}(t), \tag{119}$$

where $\hat{w}$ and $\hat{v}$ are the estimates of state variables $\bar{w}$ and $\bar{v}$. The error system is obtained by subtracting the above estimates from (99)–(102),

$$\check{w}_t(x, t) = -v^\star \check{w}_x(x, t), \tag{120}$$
$$\check{v}_t(x, t) = (\gamma p^\star - v^\star) + c(x)\check{w}(x, t), \tag{121}$$
$$\check{w}(0, t) = 0, \tag{122}$$
$$\check{v}(L, t) = \kappa \check{w}(L, t), \tag{123}$$

where $\check{w} = \bar{w} - \hat{w}$ and $\check{v} = \bar{v} - \hat{v}$. The error system is same as (79)–(82) with (89). According to Theorem 1, the error system is exponentially stable in the L^2 sense and converges to zeros in finite time t_f.

Theorem 3. *Consider system (120)–(123) with initial conditions $\check{w}_0, \check{v}_0 \in L^2[0, L]$. The equilibrium $\check{w} \equiv \check{v} \equiv 0$ is exponentially stable in the L^2 sense, which implies that $\|\bar{w}(\cdot, t) - \hat{w}(\cdot, t)\| \to 0$ and $\|\bar{v}(\cdot, t) - \hat{v}(\cdot, t)\| \to 0$. The convergence to 0 is reached in finite time $t = t_f$.*

5.3. UORM collocated boundary observer design

We define a collocated boundary measurement

$$Y_c(t) = \bar{w}(L, t). \tag{124}$$

We obtain $\bar{w}(L, t) = \left(\tilde{q}(L, t) - \rho_1 \tilde{v}(L, t)\right)/\kappa$, by the measurement of $\tilde{q}(L, t)$ and $\tilde{v}(L, t)$. Then we design a collocated boundary observer to estimate $\bar{w}(x, t)$ and $\bar{v}(x, t)$ by constructing the system

$$\hat{w}_t(x, t) = -v^\star \hat{w}_x(x, t) + r(x)(\bar{w}(L, t) - \hat{w}(L, t)), \tag{125}$$
$$\hat{v}_t(x, t) = (\gamma p^\star - v^\star)\hat{v}_x(x, t) + c(x)\hat{w}(x, t) + s(x)(\bar{w}(L, t) - \hat{w}(L, t)), \tag{126}$$
$$\hat{w}(0, t) = -k_0 \hat{v}(0, t), \tag{127}$$
$$\hat{v}(L, t) = \kappa Y_c(t) + U_{\text{out}}(t), \tag{128}$$

where $\hat{w}$ and $\hat{v}$ are the estimates of the state variables $\bar{w}$ and $\bar{v}$. The terms $r(x)$ and $s(x)$ are output injection gains to be designed. The error system is obtained by subtracting the estimates from (99)–(102),

$$\check{w}_t(x, t) = -v^\star \check{w}_x(x, t) - r(x)\check{w}(L, t), \tag{129}$$
$$\check{v}_t(x, t) = (\gamma p^\star - v^\star)\check{v}_x(x, t) + c(x)\check{w}(x, t) - s(x)\check{w}(L, t), \tag{130}$$
$$\check{w}(0, t) = -k_0 \check{v}(0, t), \tag{131}$$
$$\check{v}(L, t) = 0, \tag{132}$$

where $\check{w} = \bar{w} - \hat{w}$ and $\check{v} = \bar{v} - \hat{v}$. We need to find the output injection gains $r(x)$ and $s(x)$ that guarantee the error system decays to zero. Using backstepping transformation, we transform the error system (129)–(132) into the following system

$$\check{\lambda}_t(x, t) = -v^\star \check{\lambda}_x(x, t), \tag{133}$$
$$\check{\nu}_t(x, t) = (\gamma p^\star - v^\star)\check{\nu}_x(x, t), \tag{134}$$
$$\check{\lambda}(0, t) = -k_0 \check{\nu}(0, t), \tag{135}$$
$$\check{\nu}(L, t) = 0. \tag{136}$$

The backstepping transformation is

$$\check{\lambda}(x, t) = \check{w}(x, t) - \int_x^L \check{K}(L + x - \xi)\check{w}(\xi, t)d\xi, \tag{137}$$
$$\check{\nu}(x, t) = \check{v}(x, t) - \int_x^L \check{M}(v^\star x + (\gamma p^\star - v^\star)\xi)\check{w}(\xi, t)d\xi, \tag{138}$$

where the kernel $\check{L}$ is given by

$$\check{M}(x) = -\frac{1}{\gamma p^\star} c\left(\frac{x}{\gamma p^\star}\right). \tag{139}$$

For boundary condition (135) to hold, the kernels $\check{K}$ and $\check{M}$ satisfy the relation

$$\check{K}(L - \xi) = \check{M}((\gamma p^\star - v^\star)\xi). \tag{140}$$

the kernel $\check{K}$ is then obtained

$$\check{K}(x) = -\frac{1}{\gamma p^\star} c\left(\frac{\gamma p^\star - v^\star}{\gamma p^\star}(L - x)\right), \tag{141}$$

and

$$|\check{K}(x)| \le \frac{1}{\gamma p^\star \tau}, \tag{142}$$

according to the boundedness of $c(x)$ in (94). The output injection gains $r(x)$ and $s(x)$ are

$$r(x) = v^\star \check{K}(x) = -\frac{v^\star}{\gamma p^\star} c\left(\frac{\gamma p^\star - v^\star}{\gamma p^\star}(L-x)\right), \tag{143}$$

$$\begin{aligned} s(x) &= -v^\star \check{M}(v^\star x + (\gamma p^\star - v^\star)L) \\ &= \frac{v^\star}{\gamma p^\star} c\left(\frac{v^\star}{\gamma p^\star}x - \frac{\gamma p^\star - v^\star}{\gamma p^\star}L\right). \end{aligned} \tag{144}$$

The backstepping transformation is invertible. Therefore, we study the stability of the error system through the target system (133)–(136). It is straightforward to prove the exponential stability of error system in the L^2 sense and finite-time convergence.

Theorem 4. *Consider system (129)–(132) with inital conditions $\check{w}_0, \check{v}_0 \in L^2[0, L]$. The equilibrium $\check{w} \equiv \check{v} \equiv 0$ is exponentially stable in the L^2 sense. It holds that $\|\bar{w}(\cdot, t) - \hat{w}(\cdot, t)\| \to 0$ and $\|\bar{v}(\cdot, t) - \hat{v}(\cdot, t)\| \to 0$ and the convergence to equilibrium is reached in finite time $t = t_f$.*

We design an anti-collocated boundary observer and a collocated boundary observer. Both of them achieve the exponential stability of estimation errors in the L^2 sense and finite-time convergence to 0. In comparison, the collocated boundary observer needs two spatially varying output injection gains, but could be easier to install in practice since it is located at the same boundary with UORM controller $U_{\text{out}}(t)$.

5.4. UORM output feedback control design

Combining the state feedback controller and the boundary observers, we have the output feedback controller

$$\begin{aligned} U_{\text{out}}(t) = &-\kappa \hat{w}(L, t) + \int_0^L M(L-\xi)\hat{v}(\xi, t)d\xi \\ &+ \int_0^L K(L, \xi)\hat{w}(\xi, t)d\xi, \end{aligned} \tag{145}$$

where $\hat{w}$ and $\hat{v}$ can be obtained from the anti-collocated boundary observer in (116)–(119) with measurement $Y_a(t) = \bar{v}(0, t)$ or from the collocated boundary observer in (129)–(132) with measurement $Y_c(t) = \bar{w}(L, t)$ and observer gains given in (143), (144). The following theorem summarizes the results from Theorems 2–4.

Theorem 5. *Consider system (99)–(102) with inital conditions $\hat{w}_0, \hat{v}_0 \in L^2[0, L]$ and with output feed control law (145), where the kernels $K(x, \xi)$, $M(x)$ are obtained by solving (109)–(111). The equilibrium $\bar{w} \equiv \bar{v} \equiv \hat{w} \equiv \hat{v} \equiv 0$ is exponentially stable in the L^2 sense.*

6. Adaptive UORM control design

The previous feedback control designs are based on the knowledge of parameters in the system. However, the relaxation time τ is hard to measure in practice and is affected by many factors. In addition, coefficient γ in the pressure–density relation reflects the aggressiveness of drivers' behavior and relates to road situation. Due to the change of road at inlet or outlet with on-ramp, values of γ are different for in-domain and boundaries. We consider γ to be unknown at boundaries but a known coefficient within the domain $\mathscr{U}$. According to (36), k_0 is considered as an unknown constant parameter at boundary. The adaptive control law that is proposed in this section can also be used as an alternative non-adaptive output feedback control design if parameters are given.

Consider the following hyperbolic system with adaptive control input $U(t)$,

$$\bar{w}_t(x, t) = -v^\star \bar{w}_x(x, t), \tag{146}$$

$$\bar{v}_t(x, t) = (\gamma p^\star - v^\star)\bar{v}_x(x, t) + c(x)\bar{w}(x, t), \tag{147}$$

$$\bar{w}(0, t) = -k_0 \bar{v}(0, t), \tag{148}$$

$$\bar{v}(L, t) = \kappa \bar{w}(L, t) + U(t), \tag{149}$$

with the measurement $Y(t)$ at the inlet and by (25),

$$Y(t) = \tilde{v}(0, t), \tag{150}$$

$$\bar{v}(0, t) = \rho_2 Y(t), \tag{151}$$

where $x \in \mathscr{U} \triangleq [0, L]$ and $t > 0$. The coefficients k_0, ρ_2 and $\kappa = \exp\left(\frac{-L}{\tau v^\star}\right)$ are unknown constant boundary parameters and $c(x) = -\frac{1}{\tau}\exp\left(-\frac{x}{\tau v^\star}\right)$ is unknown spatially-varying parameter, since τ is unknown. The steady states $p^\star$, $q^\star$ and $v^\star$ are known.

6.1. Scaling the states

First we scale $\bar{w}$ with unknown constant κ and $\bar{v}$ with unknown constant k_2 for the convenience of the parameter estimation,

$$\omega(x, t) = \frac{\kappa}{\rho_2}\bar{w}(x, t), \tag{152}$$

$$\tilde{v}(x, t) = \frac{1}{\rho_2}\bar{v}(x, t), \tag{153}$$

and the system is mapped into

$$\omega_t(x, t) = -v^\star \omega_x(x, t), \tag{154}$$

$$\tilde{v}_t(x, t) = (\gamma p^\star - v^\star)\tilde{v}_x(x, t) + \bar{c}(x)\omega(x, t), \tag{155}$$

$$\omega(0, t) = -\kappa k_0 \tilde{v}(0, t), \tag{156}$$

$$\tilde{v}(L, t) = \omega(L, t) + \frac{1}{\rho_2}U(t), \tag{157}$$

where the unknown parameters are defined as

$$\bar{c}(x) = \frac{c(x)}{\kappa}, \quad r_0 = -\kappa k_0, \quad r_1 = \frac{1}{\rho_2}, \tag{158}$$

with measurement $\tilde{v}(0, t) = Y(t)$. The scaling of $\bar{w}$ and $\bar{v}$ reduces the number of couplings between unknown coefficients and state variables.

6.2. Observer canonical form

In order to decouple the $(\omega, \tilde{v})$-system in domain, we use the following backstepping transformation.

$$\alpha(x, t) = \omega(x, t) - \int_0^x \bar{M}(x-\xi)\omega(\xi, t)d\xi, \tag{159}$$

$$\beta(x, t) = \tilde{v}(x, t) - \int_0^x \bar{K}(v^\star x + (\gamma p^\star - v^\star)\xi)\omega(\xi, t)d\xi. \tag{160}$$

We transform the $(\omega, \tilde{v})$-system into an observer canonical form,

$$\alpha_t(x, t) = -v^\star \alpha_x(x, t) + \theta_1(x)Y(t), \tag{161}$$

$$\beta_t(x, t) = (\gamma p^\star - v^\star)\beta_x(x, t) + \theta_2(x)Y(t) \tag{162}$$

$$\alpha(0, t) = r_0 \beta(0, t), \tag{163}$$

$$\beta(L, t) = \alpha(L, t) + r_1 U(t), \tag{164}$$

where $\theta_1(x) = -v^\star r_0 \bar{M}(x)$ and $\theta_2(x) = -v^\star r_0 \bar{K}(v^\star x)$. The measurement is

$$\alpha(0, t) = r_0 Y(t), \tag{165}$$

$$\beta(0, t) = Y(t). \tag{166}$$

To obtain the target system, we take the time and spatial derivatives on both sides of (159), (160). The kernels are

$$\bar{M}(x) = -\frac{1}{\gamma p^\star}\bar{c}\left(L - \frac{\gamma p^\star - v^\star}{\gamma p^\star}x\right), \quad \bar{K}(x) = -\frac{1}{\gamma p^\star}\bar{c}\left(\frac{x}{\gamma p^\star}\right), \tag{167}$$

and new spatial parameters are

$$\theta_1(x) = \frac{r_0 v^\star}{\gamma p^\star}\bar{c}\left(L - \frac{\gamma p^\star - v^\star}{\gamma p^\star}x\right), \quad \theta_2(x) = \frac{r_0 v^\star}{\gamma p^\star}\bar{c}\left(\frac{v^\star}{\gamma p^\star}x\right). \tag{168}$$

Remark 6. For $\forall x \in [0, L]$, the following holds for $\Theta \triangleq \frac{\gamma p^\star - v^\star}{\gamma p^\star \tau}$,

$$|\theta_1(x)| \le \Theta, \quad |\theta_2(x)| \le \Theta. \tag{169}$$

6.3. Parametric model and parameter estimation

We can easily find the input/output relation for the observer canonical form by solving the system (161)–(164) directly,

$$\alpha(x,t) = \begin{cases} \alpha(x - v^\star t, 0) + \displaystyle\int_0^t \theta_1(x - v^\star(t-s))Y(s)ds, \\ \qquad\qquad t < \dfrac{x}{v^\star}, \\ \alpha\left(0, t - \dfrac{x}{v^\star}\right) + \dfrac{1}{v^\star}\displaystyle\int_0^x \theta_1(s)Y\left(t - \dfrac{x-s}{v^\star}\right)ds, \\ \qquad\qquad t \ge \dfrac{x}{v^\star}. \end{cases} \tag{170}$$

Substituting into $\alpha(0,t) = r_0 Y(t)$ and therefore we find, for $t \ge \frac{x}{v^\star}$:

$$\alpha(x,t) = r_0 Y\left(t - \frac{x}{v^\star}\right) + \frac{1}{v^\star}\int_0^x \theta_1(s)Y\left(t - \frac{x-s}{v^\star}\right)ds. \tag{171}$$

Thus we can obtain $\alpha(L,t)$ by the knowledge of $Y(t)$ from $t - \frac{L}{v^\star}$ to t,

$$\alpha(L,t) = r_0 Y\left(t - \frac{L}{v^\star}\right) + \frac{1}{v^\star}\int_0^L \theta_1(s)Y\left(t - \frac{L-s}{v^\star}\right)ds. \tag{172}$$

Given $\beta(L,t) = \alpha(L,t) + r_1 U(t)$, we solve for $\beta(x,t)$,

$$\beta(x,t) = \begin{cases} \beta(x + (\gamma p^\star - v^\star)t, 0) \\ \quad + \displaystyle\int_0^t \theta_2(x + (\gamma p^\star - v^\star)(t-s))Y(s)ds, \\ \qquad\qquad t < \dfrac{L-x}{\gamma p^\star - v^\star}, \\ \beta\left(L, t - \dfrac{L-x}{\gamma p^\star - v^\star}\right) \\ \quad + \dfrac{1}{\gamma p^\star - v^\star}\displaystyle\int_x^L \theta_2(s)Y\left(t - \dfrac{s-x}{\gamma p^\star - v^\star}\right)ds, \\ \qquad\qquad t \ge \dfrac{L-x}{\gamma p^\star - v^\star}. \end{cases} \tag{173}$$

We now find for $t \ge \frac{L-x}{\gamma p^\star - v^\star}$:

$$\begin{aligned}\beta(x,t) =& \beta\left(L, t - \frac{L-x}{\gamma p^\star - v^\star}\right) \\ &+ \frac{1}{\gamma p^\star - v^\star}\int_x^L \theta_2(s)Y\left(t - \frac{s-x}{\gamma p^\star - v^\star}\right)ds,\end{aligned} \tag{174}$$

thus for $t \ge \frac{L}{\gamma p^\star - v^\star}$, we have

$$\begin{aligned}\beta(0,t) =& \alpha\left(L, t - \frac{L}{\gamma p^\star - v^\star}\right) + r_1 U\left(t - \frac{L}{\gamma p^\star - v^\star}\right) \\ &+ \frac{1}{\gamma p^\star - v^\star}\int_0^L \theta_2(s)Y\left(t - \frac{s}{\gamma p^\star - v^\star}\right)ds.\end{aligned} \tag{175}$$

By substituting $\alpha(L,t)$ in $Y(t)$, we obtain the input/output parametric model,

$$\begin{aligned}Y(t) =& r_1 U\left(t - \frac{L}{\gamma p^\star - v^\star}\right) + r_0 Y\left(t - \frac{L}{v^\star} - \frac{L}{\gamma p^\star - v^\star}\right) \\ &+ \int_{t - \frac{L}{v^\star} - \frac{L}{\gamma p^\star - v^\star}}^{t - \frac{L}{\gamma p^\star - v^\star}} \theta_1\left(v^\star(s-t) + \frac{\gamma p^\star}{\gamma p^\star - v^\star}L\right)Y(s)ds \\ &- \int_{t - \frac{L}{\gamma p^\star - v^\star}}^{t} \theta_2\left((\gamma p^\star - v^\star)(t-s)\right)Y(s)ds + \varepsilon(t),\end{aligned} \tag{176}$$

where $\varepsilon(t)$ is defined as the error of the parametric model. The value of $\varepsilon(t)$ is arbitrary for $t \in [0, \frac{L}{v^\star} + \frac{L}{\gamma p^\star - v^\star}]$, depending on the initial values of $\alpha(x,0)$, $\beta(x,0)$ and $\varepsilon(t) = 0$ for $t \in [\frac{L}{v^\star} + \frac{L}{\gamma p^\star - v^\star}, \infty)$. We use this input/output parametric model to estimate the unknown spatially-varying parameters $\theta_1(x)$, $\theta_2(x)$ and unknown constant boundary parameter r_0.

The following update laws are based on the gradient algorithm with normalization and projection,

$$\partial_t \hat{\theta}_1(x) = \text{Proj}\left(\tau_1(x,t), \hat{\theta}_1(x,t)\right), \tag{177}$$

$$\partial_t \hat{\theta}_2(x) = \text{Proj}\left(\tau_2(x,t), \hat{\theta}_2(x,t)\right), \tag{178}$$

$$\partial_t \hat{r}_0 = \frac{\gamma_3}{\sigma(t)}Y\left(t - \frac{L}{v^\star} - \frac{L}{\gamma p^\star - v^\star}\right)\tilde{\beta}(0,t), \tag{179}$$

$$\partial_t \hat{r}_1 = \frac{\gamma_4}{\sigma(t)}U\left(t - \frac{L}{\gamma p^\star - v^\star}\right)\tilde{\beta}(0,t), \tag{180}$$

where $\gamma_1(x)$, $\gamma_2(x)$, γ_3 and γ_4 are positive adaptation gains and

$$\tau_1(x,t) = \frac{\gamma_1(x)Y\left(t - \frac{L-x}{v^\star} - \frac{L}{\gamma p^\star - v^\star}\right)}{\sigma(t)v^\star}\tilde{\beta}(0,t), \tag{181}$$

$$\tau_2(x,t) = \frac{\gamma_2(x)Y\left(t - \frac{x}{\gamma p^\star - v^\star}\right)}{\sigma(t)(\gamma p^\star - v^\star)}\tilde{\beta}(0,t). \tag{182}$$

The normalization is given by

$$\begin{aligned}\sigma(t) =& 1 + Y^2\left(t - \frac{L}{v^\star} - \frac{L}{\gamma p^\star - v^\star}\right) + U^2\left(t - \frac{L}{\gamma p^\star - v^\star}\right) \\ &+ \int_{t - \frac{L}{v^\star} - \frac{L}{\gamma p^\star - v^\star}}^{t} Y^2(s)ds.\end{aligned} \tag{183}$$

The adaptive estimation error $\tilde{\beta}(0,t)$ of parameter estimates $\hat{\theta}_1(x)$, $\hat{\theta}_2(x)$, $\hat{r}_0$ and $\hat{r}_1$ is obtained from the input/output parametric model as follows,

$$\begin{aligned}\tilde{\beta}(0,t) =& \beta(0,t) - \hat{\beta}(0,t) \\ =& Y(t) - \hat{r}_1 U\left(t - \frac{L}{\gamma p^\star - v^\star}\right) \\ &- \hat{r}_0 Y\left(t - \frac{L}{v^\star} - \frac{L}{\gamma p^\star - v^\star}\right) \\ &+ \int_{t - \frac{L}{v^\star} - \frac{L}{\gamma p^\star - v^\star}}^{t - \frac{L}{\gamma p^\star - v^\star}} \hat{\theta}_1\left(v^\star(s-t) + \frac{\gamma p^\star}{\gamma p^\star - v^\star}L\right)Y(s)ds \\ &- \int_{t - \frac{L}{\gamma p^\star - v^\star}}^{t} \hat{\theta}_2\left((\gamma p^\star - v^\star)(t-s)\right)Y(s)ds - \varepsilon(t).\end{aligned} \tag{184}$$

The projection operator is given by

$$\text{Proj}(\tau_i, \hat{\theta}_i) = \begin{cases} \tau_i, & |\hat{\theta}_i| < \Theta \quad \text{or} \quad \hat{\theta}_i \tau_i \le 0, \\ 0, & |\hat{\theta}_i| = \Theta \quad \text{and} \quad \hat{\theta}_i \tau_i > 0. \end{cases} \tag{185}$$

Denote the parameter estimation errors as

$$\tilde{\theta}_i(x,t) = \theta_i(x) - \hat{\theta}_i(x,t), \quad i = 1,2 \tag{186}$$
$$\tilde{r}_j(t) = r_j - \hat{r}_j(t), \quad j = 0,1. \tag{187}$$

Lemma 7. *The update laws (177)–(179) guarantee that:*

$$|\hat{\theta}_1(x)| \le \Theta, |\hat{\theta}_2(x)| \le \Theta, \tag{188}$$
$$\|\widetilde{\theta}_1\|, \|\widetilde{\theta}_2\|, \widetilde{r}_0, \widetilde{r}_1 \in \mathscr{L}_\infty, \tag{189}$$
$$\|\partial_t \hat{\theta}_1\|, \|\partial_t \hat{\theta}_2\|, \partial_t \hat{r}_0, \partial_t \hat{r}_1, \frac{\tilde{\beta}(0,t)}{\sqrt{\sigma(t)}} \in \mathscr{L}_2 \cap \mathscr{L}_\infty. \tag{190}$$

By constructing Lyapunov function for the adaptive estimation errors $\tilde{\theta}_i$ and $\tilde{r}_j$, it is straightforward to prove the above lemma. The detailed proof is omitted here. The projection in (185) guarantees that $\theta_1(x)$, $\theta_2(x)$ are pointwise bounded not only L^2 bounded, as shown in (188).

6.4. Filter-based observer design

We introduce the adaptive state estimates based on the input and output filters,

$$\hat{\alpha}(x,t) = \hat{r}_0 \phi_1(x,t) + \frac{1}{v^\star}\int_0^x \hat{\theta}_1(\xi)\phi_1(x-\xi,t)d\xi, \tag{191}$$
$$\hat{\beta}(x,t) = \hat{\psi}(x,t) + \frac{1}{\gamma p^\star - v^\star}\int_x^L \hat{\theta}_2(\xi)\phi_2(L+x-\xi,t)d\xi. \tag{192}$$

We represent the signal $\hat{\beta}(L,t)$, the output $Y(t)$ with the following transport PDEs. The filter for $\hat{\beta}(L,t)$ is

$$\hat{\psi}_t(x,t) = (\gamma p^\star - v^\star)\hat{\psi}_x(x,t), \tag{193}$$
$$\hat{\psi}(L,t) = \hat{\beta}(L,t), \quad \hat{\psi}(x,0) = \hat{\psi}_0(x), \tag{194}$$

where $\hat{\beta}(L,t) = \hat{r}_1 U(t) + \hat{\alpha}(L,t)$. The signal $\hat{\alpha}(L,t)$ is obtained from (172) with updated parameters $\hat{\theta}_1(x,t)$ and $\hat{r}_1(t)$,

$$\hat{\alpha}(L,t) = \hat{r}_0 Y\left(t - \frac{L}{v^\star}\right) + \frac{1}{v^\star}\int_0^L \hat{\theta}_1(s) Y\left(t - \frac{L-s}{v^\star}\right) ds. \tag{195}$$

The filters for $Y(t)$ are

$$\partial_t \phi_1(x,t) = -v^\star \partial_x \phi_1(x,t), \tag{196}$$
$$\phi_1(0,t) = Y(t), \quad \phi_1(x,0) = \phi_{10}(x), \tag{197}$$

and

$$\partial_t \phi_2(x,t) = (\gamma p^\star - v^\star)\partial_x \phi_2(x,t), \tag{198}$$
$$\phi_2(L,t) = Y(t), \quad \phi_2(x,0) = \phi_{20}(x), \tag{199}$$

where $x \in [0,L]$, and $\hat{\psi}_0, \phi_{10}, \phi_{20}$ are arbitrary initial conditions verifying boundary conditions. The explicit solutions to the above PDE filters for $t > \max\left(\frac{L}{v^\star}, \frac{L}{\gamma p^\star - v^\star}\right)$ are given by

$$\hat{\psi}(x,t) = \hat{r}_1 U\left(t - \frac{L-x}{\gamma p^\star - v^\star}\right) + \hat{\alpha}\left(L, t - \frac{L-x}{\gamma p^\star - v^\star}\right), \tag{200}$$
$$\phi_1(x,t) = Y\left(t - \frac{x}{v^\star}\right), \tag{201}$$
$$\phi_2(x,t) = Y\left(t - \frac{L-x}{\gamma p^\star - v^\star}\right). \tag{202}$$

The adaptive estimates $\hat{\alpha}(x,t)$ and $\hat{\beta}(x,t)$ verify that

$$\hat{\alpha}_t = -v^\star \hat{\alpha}_x + \hat{\theta}_1(x)Y(t) + \hat{r}_{0t}\phi_1(x,t) + \frac{1}{v^\star}\int_0^x \partial_t \hat{\theta}_1(\xi)\phi_1(x-\xi,t)d\xi, \tag{203}$$

$$\hat{\beta}_t = (\gamma p^\star - v^\star)\hat{\beta}_x + \hat{\theta}_2(x)Y(t) + \frac{1}{\gamma p^\star - v^\star}\int_x^L \partial_t \hat{\theta}_2(\xi)\phi_2(L+x-\xi,t)d\xi, \tag{204}$$

with boundary conditions

$$\hat{\alpha}(0,t) = \hat{r}_0\phi_1(0,t) = \hat{r}_0 Y(t), \tag{205}$$
$$\hat{\beta}(L,t) = \hat{\psi}(L,t) = \hat{r}_1 U(t) + \hat{\alpha}(L,t). \tag{206}$$

Denote the adaptive observer errors as

$$\tilde{\alpha} = \alpha - \hat{\alpha}, \quad \tilde{\beta} = \beta - \hat{\beta}, \tag{207}$$

The error system is governed by

$$\tilde{\alpha}_t = -v^\star \tilde{\alpha}_x + \tilde{\theta}_1(x)Y(t) - \hat{r}_{0t}\phi_1(x,t) - \frac{1}{v^\star}\int_0^x \partial_t \hat{\theta}_1(\xi)\phi_1(x-\xi,t)d\xi, \tag{208}$$

$$\tilde{\beta}_t = (\gamma p^\star - v^\star)\tilde{\beta}_x + \tilde{\theta}_2(x)Y(t) - \frac{1}{\gamma p^\star - v^\star}\int_x^L \partial_t \hat{\theta}_2(\xi)\phi_2(L+x-\xi,t)d\xi, \tag{209}$$

with boundary conditions

$$\tilde{\alpha}(0,t) = \tilde{r}_0 Y(t), \tag{210}$$
$$\tilde{\beta}(L,t) = \tilde{r}_1 U(t) + \tilde{\alpha}(L,t). \tag{211}$$

6.5. Adaptive output feedback control design

To obtain the adaptive control law, we apply the backstepping transformation to the adaptive state estimate $\hat{\beta}$. The transformed state is given by

$$\eta(x) = \hat{\beta}(x) - \frac{1}{\gamma p^\star - v^\star}\int_0^x \hat{K}_2(x-\xi)\hat{\beta}(\xi)d\xi \triangleq \mathscr{F}[\hat{\beta}](x), \tag{212}$$

where $\hat{K}_2$ is obtained by solving online the following Volterra equation,

$$\hat{K}_2(x) = -\hat{\theta}_2(x) + \frac{1}{\gamma p^\star - v^\star}\int_0^x \hat{K}_2(x-\xi)\hat{\theta}_2(\xi)d\xi. \tag{213}$$

Note that $\hat{K}_2(x)$ and $\hat{\theta}_2(x)$ are functions of time. The inverse transformation is then given by

$$\hat{\beta}(x) = \eta(x) - \frac{1}{\gamma p^\star - v^\star}\int_0^x \hat{\theta}_2(x-\xi)\hat{\eta}(\xi)d\xi \triangleq \hat{\eta} - \frac{1}{\gamma p^\star - v^\star}\hat{\theta}_2 * \hat{\eta}. \tag{214}$$

With a lengthy but straightforward calculation, we obtain that

$$\eta_t = (\gamma p^\star - v^\star)\eta_x - \hat{K}_2(x)\tilde{\beta}(0) + \eta * \mathscr{F}[\partial_t \hat{\theta}_2](x) + \frac{1}{\gamma p^\star - v^\star}\left(\int_x^L \partial_t \hat{\theta}_2(\xi)\phi_2(L+x-\xi,t)d\xi\right), \tag{215}$$
$$\eta(L) = 0, \tag{216}$$

and the adaptive control law is derived from (216).

We summarize the transformation and inverse transformation between the original system $(\bar{w}, \bar{v}, \hat{\psi}, \phi_1, \phi_2)$ and the final target system $(\tilde{\alpha}, \tilde{\beta}, \hat{\zeta}, \hat{\eta}, \phi_1, \phi_2)$ as:

$$\phi_1 = \phi_1, \phi_2 = \phi_2, \tag{217}$$
$$\hat{\alpha} = \mathscr{T}_\alpha[\phi_1], \eta = (\mathscr{I} - \mathscr{F})[\hat{\psi} + \mathscr{T}_\beta[\phi_2]], \tag{218}$$
$$\tilde{\beta} = (\mathscr{I} - \mathscr{G})[\bar{v}/k_2] - (\hat{\psi} + \mathscr{T}_\beta[\phi_2]), \tag{219}$$
$$\tilde{\alpha} = (\mathscr{I} - \mathscr{G})[-\kappa\bar{w}] - \mathscr{T}_\alpha[\phi_1], \tag{220}$$

and we can obtain the original states from the inverse transformation as:

$$\phi_1 = \phi_1, \phi_2 = \phi_2, \tag{221}$$

$$\hat{\psi} = \eta - \frac{1}{v^\star}\hat{\theta}_2 * \eta - \mathscr{T}_\beta[\phi_2], \tag{222}$$

$$\bar{w} = -\frac{1}{\kappa}(\mathscr{I} - \mathscr{G})^{-1}[\tilde{\alpha} + \hat{\alpha}], \tag{223}$$

$$\bar{v} = k_2(\mathscr{I} - \mathscr{G})^{-1}[\tilde{\beta} + \hat{\psi} + \mathscr{T}_\beta[\phi_2]]. \tag{224}$$

Due to the invertibility of the above transformation, we can obtain the stability of the original system $(\bar{w}, \bar{v}, \hat{\psi}, \phi_1, \phi_2)$ by studying the system in the equivalent variables $(\tilde{\alpha}, \tilde{\beta}, \hat{\alpha}, \eta, \phi_1, \phi_2)$. The target system $(\tilde{\alpha}, \tilde{\beta}, \hat{\alpha}, \eta, \phi_1, \phi_2)$ is governed by the following PDEs,

$$\begin{aligned}\tilde{\alpha}_t =& -v^\star\tilde{\alpha}_x + \tilde{\theta}_1(x)Y(t) - \hat{r}_{0t}\phi_1(x,t)\\ &- \frac{1}{v^\star}\int_0^x \partial_t\hat{\theta}_1(\xi)\phi_1(x-\xi,t)d\xi,\end{aligned} \tag{225}$$

$$\tilde{\alpha}(0,t) = \tilde{r}_0 Y(t), \tag{226}$$

$$\begin{aligned}\tilde{\beta}_t =& (\gamma p^\star - v^\star)\tilde{\beta}_x + \tilde{\theta}_2(x)Y(t)\\ &- \frac{1}{\gamma p^\star - v^\star}\int_x^L \partial_t\hat{\theta}_2(\xi)\phi_2(L+x-\xi,t)d\xi,\end{aligned} \tag{227}$$

$$\tilde{\beta}(L,t) = \tilde{\alpha}(L,t) + \tilde{r}_1 U(t), \tag{228}$$

$$\begin{aligned}\hat{\alpha}_t =& -v^\star\hat{\alpha}_x + \hat{\theta}_1(x)Y(t) + \hat{r}_{0t}\phi_1(x,t)\\ &+ \frac{1}{v^\star}\int_0^x \partial_t\hat{\theta}_1(\xi)\phi_1(x-\xi,t)d\xi,\end{aligned} \tag{229}$$

$$\hat{\alpha}(0,t) = \hat{r}_0 Y(t), \tag{230}$$

$$\begin{aligned}\eta_t =& (\gamma p^\star - v^\star)\eta_x - \hat{K}_2(x)\tilde{\beta}(0) + \eta * \mathscr{F}[\partial_t\hat{\theta}_2](x)\\ &+ \frac{1}{\gamma p^\star - v^\star}\mathscr{F}\left[\int_x^L \partial_t\hat{\theta}_2(\xi)\phi_2(L+x-\xi,t)d\xi\right],\end{aligned} \tag{231}$$

$$\eta(L,t) = 0, \tag{232}$$

$$\partial_t\phi_2(x,t) = (\gamma p^\star - v^\star)\partial_x\phi_2(x,t), \tag{233}$$

$$\phi_2(L,t) = Y(t), \tag{234}$$

$$\partial_t\phi_1(x,t) = -v^\star\partial_x\phi_1(x,t), \tag{235}$$

$$\phi_1(0,t) = Y(t). \tag{236}$$

Note that $Y(t) = \eta(0) + \tilde{\beta}(0)$. According to backstepping transformation (212), we can obtain from (232) that

$$\hat{\beta}(L,t) = \int_0^L \hat{K}_2(L-\xi)\hat{\beta}(\xi,t)d\xi. \tag{237}$$

Substituting $\hat{\beta}(L,t) = \hat{r}_1 U(t) + \hat{\alpha}(L,t)$, we have

$$U(t) = \frac{1}{\hat{r}_1}\int_0^L \hat{K}_2(L-\xi)\hat{\beta}(\xi,t)d\xi - \frac{1}{\hat{r}_1}\hat{\alpha}(L,t). \tag{238}$$

Using the adaptive estimates $\hat{\beta}(x,t)$ in (192) and $\hat{\alpha}(L,t)$ in (195), the adaptive controller is then obtained in an explicit integral form, consisting delayed values of input and output,

$$\begin{aligned}U(t) =& \frac{1}{\hat{r}_1}\int_{t-\frac{L}{\gamma p^\star - v^\star}}^t \hat{K}_2\left(v^\star(t-\xi)\right)U(\xi)d\xi\\ &- \frac{\hat{r}_0}{\hat{r}_1}\hat{Y}\left(t - \frac{L}{v^\star}\right) - \frac{1}{\hat{r}_1}\int_{t-\frac{L}{v^\star}}^t m_1(\xi)Y(\xi)d\xi\\ &+ \frac{\hat{r}_0}{\hat{r}_1}\int_{t-\frac{L}{v^\star}-\frac{L}{\gamma p^\star - v^\star}}^{t-\frac{L}{v^\star}} m_2(\xi)Y(\xi)d\xi\end{aligned}$$

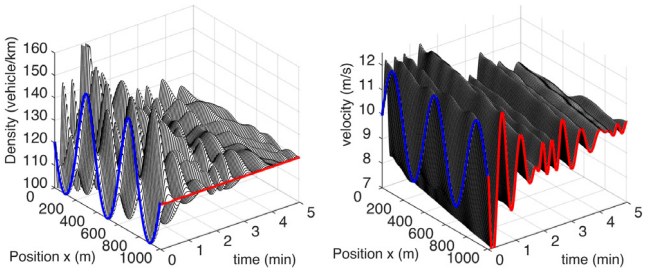

Fig. 5. Open-loop system.

$$\begin{aligned}&+ \frac{1}{\hat{r}_1}\int_{t-\frac{L}{\gamma p^\star - v^\star}}^t m_3(\xi)\int_{\xi-\frac{L}{v^\star}}^{\xi} m_4(\mu)Y(\mu)d\mu d\xi\\ &+ \frac{1}{\hat{r}_1}\int_{t-\frac{L}{\gamma p^\star - v^\star}}^t m_5(\xi)Y(\xi)d\xi,\end{aligned} \tag{239}$$

where m_i are denoted as

$$m_1(\xi) = \hat{\theta}_1(L - v^\star(t-\xi)), \tag{240}$$

$$m_2(\xi) = \hat{K}_2\left(\left(\gamma p^\star - v^\star\right)\left(t - \xi - \frac{L}{v^\star}\right)\right), \tag{241}$$

$$m_3(\xi) = \hat{K}_2\left((\gamma p^\star - v^\star)(t-\xi)\right), \tag{242}$$

$$m_4(\mu) = \hat{\theta}_1\left(L - v^\star(\xi - \mu)\right), \tag{243}$$

$$m_5(\xi) = \int_{(\gamma p^\star - v^\star)(t-\xi)}^L \hat{K}_2(\mu)\hat{\theta}_2((\gamma p^\star - v^\star)(t-\xi) + L - \mu)d\mu. \tag{244}$$

The parameter estimates $\hat{\theta}_1(x,t)$, $\hat{\theta}_2(x,t)$, $\hat{r}_0$ and $\hat{r}_1$ are generated from the update laws. We can obtain $\hat{K}_2(x,t)$ by solving online the Volterra equation in (213). The Lyapunov stability proof is shown in Appendix, which is derived from modifications of the proof in Yu et al. (2017). The key idea in proving the stability of $(\tilde{\alpha}, \tilde{\beta}, \hat{\alpha}, \eta, \phi_1, \phi_2)$-system is to take advantage of the cascade structure of the system. Due to the invertibility between $(\tilde{q}, \tilde{v})$-system and $(\bar{w}, \bar{v})$-system, we arrive our main theorem for adaptive control design.

Theorem 8. *Consider the plant (146)–(149) with the adaptive control law (239) and update laws (177)–(179). For any initial conditions $\hat{\theta}_1(\cdot,0), \hat{\theta}_2(\cdot,0), r_0(0), r_1(0) \in \mathscr{C}^1[0,L]$, $\bar{w}_0, \bar{v}_0, \phi_{10}, \phi_{20}, \hat{\psi}_0$ that verify boundary conditions, the solution $(\bar{w}, \bar{v}, \phi_1, \phi_2, \hat{\psi}, \hat{\theta}_1, \hat{\theta}_2, \hat{r}_0, \hat{r}_1)$ is bounded for $t \geq 0$ and for $\forall x \in [0,L]$ it verifies that as $t \to \infty$,*

$$\|\bar{w}(x,t)\| \to 0, \|\bar{v}(x,t)\| \to 0, \tag{245}$$

$$\|\tilde{q}(x,t)\| \to 0, \|\tilde{v}(x,t)\| \to 0. \tag{246}$$

7. Simulation

We take $\gamma = 1$. The length of freeway section is chosen to be $L = 1$ km. The free speed is $v_f = 40$ m/s and the maximum density is $\rho_m = 150$ vehicles/km. The steady states $(\rho^\star, v^\star)$ are chosen as (120 vehicles/km, 10 m/s) which is in the congested regime. The relaxation time $\tau = 60$ s. We use sinusoid initial conditions.

Fig. 5 shows that in the open-loop system the density and velocity are slightly damped and keeps oscillating. In Fig. 6, the closed-loop system with DORM control is stabilized and converges to the steady states in the finite time about 2.5 min. The closed-loop system with UORM full-state feedback control in Fig. 7 is stabilized and converges to the reference and the finite convergence time is $t_f = L/v^\star + L/(\gamma p^\star - v^\star) = 150$ s $= 2.5$ min.

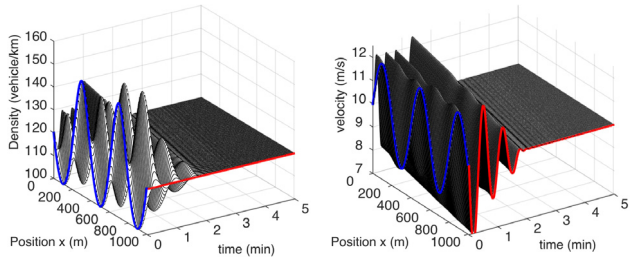

Fig. 6. Closed-loop system with DORM control.

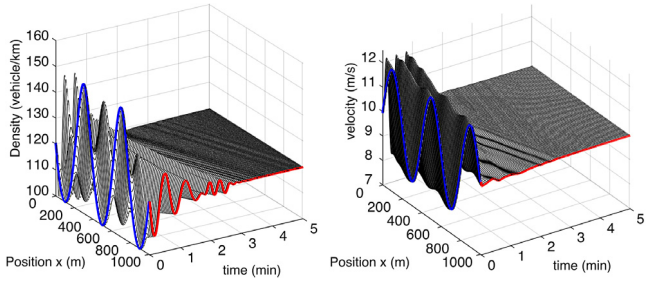

Fig. 7. Closed-loop system with UORM full-state feedback.

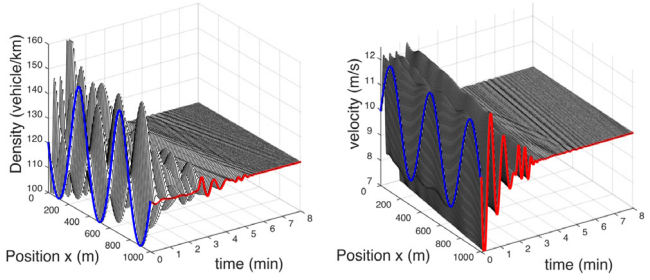

Fig. 8. Closed-loop system with UORM output feedback.

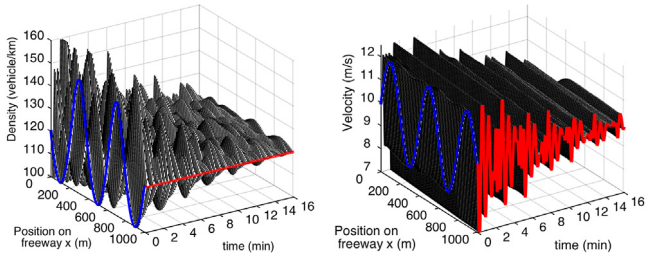

Fig. 9. Open-loop system without adaptive UORM output feedback.

The evolution of ramp metering control input is plotted with red color at outlet $x = 1000$ m. We see the control input oscillates around every half minute, which is reasonable in application. Fig. 8 shows that the closed-loop system with UORM output feedback control (collocated observer) is stabilized and converges to the steady states in about 5 min since it takes the collocated observer 2.5 min to estimate state variables and another 2.5 min for state feedback control to converge to the steady states.

In the adaptive simulation, we choose $\tau = 100$ s. The open-loop system is more oscillated than that of the non-adaptive case. It takes longer time to stabilize with adaptive output feedback control law. In Fig. 9, we can see that the open-loop system is unstable. The adaptive output feedback result is shown in Fig. 10.

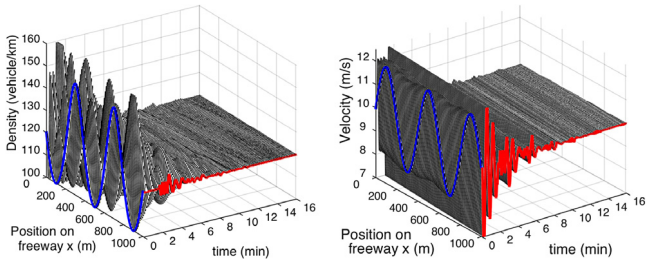

Fig. 10. Closed-loop system with adaptive UORM output feedback.

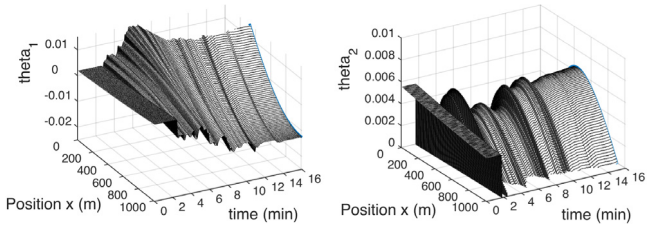

Fig. 11. Estimates of spatially-varying parameters.

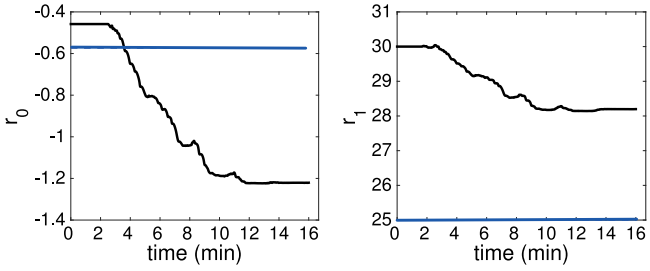

Fig. 12. Estimates of constant parameters.

The estimation of parameters in the system is given in Figs. 11 and 12. The blue lines in Fig. 12 represent the true values of the constant parameters. The parameter estimates do not necessarily converge to the true values, due to the local property of gradient methods.

8. Conclusion

This paper addresses the boundary feedback control problem of ARZ traffic model with relaxation term. To stabilize the oscillations of congested traffic regime, two control designs are introduced for the second-order coupled hyperbolic system. The key idea in the DORM control design is to cancel the forward coupling in the system. In the harder case, UORM control design uses backstepping method to cancel the coupling at outlet and thus achieves exponential stability and finite time convergence to the steady states. In the absence of parameters knowledge, we solve adaptive boundary control problem of linearized ARZ model using backstepping method, gradient-based update laws and a filter-based approach. The main step is to develop upstream of ramp metering control approach and transform the hetero-directional coupled hyperbolic system to the observer canonical form that is suitable for adaptive design. It is of interest to explore adaptive control design for this problem without over-parameterization and more research is needed to be done on the property of relaxation time in the ARZ model. A useful extension is to consider the effect of changing lanes and autonomous vehicles in traffic model.

Appendix. Proof of Theorem 8

A.1. L_2 boundedness

The boundedness of $\hat{\theta}_2$ is given by Lemma 7. Using (213) and Gronwall's inequality, we establish a bound on $\hat{K}_2$,

$$|\hat{K}_2(x)| \leq \Theta e^{\frac{\Theta}{\gamma p^\star - v^\star}} \triangleq K_2. \tag{A.1}$$

To prove the L_2 boundedness of system in (225)–(236), we construct the following Lyapunov functions:

$$V_1 = \frac{1}{2}\int_0^L e^{-x}\tilde{\alpha}^2(x)dx, \quad V_2 = \frac{1}{2}\int_0^L e^{x}\tilde{\beta}^2(x)dx, \tag{A.2}$$

$$V_3 = \frac{1}{2}\int_0^L e^{-x}\hat{\alpha}^2(x)dx, \quad V_4 = \frac{1}{2}\int_0^L e^{x}\eta^2(x)dx, \tag{A.3}$$

$$V_5 = \frac{1}{2}\int_0^L e^{x}\phi_1^2(x)dx \quad V_6 = \frac{1}{2}\int_0^L e^{x}\phi_2^2(x)dx. \tag{A.4}$$

Then we get

$$\begin{aligned}\dot{V}_1 \leq & -\frac{v^\star}{2e^L}\tilde{\alpha}^2(L) - \frac{1}{2}\left(\frac{v^\star}{e^L} - \frac{c_1}{v^\star} - c_2\right)\|\tilde{\alpha}\|^2 \\ & + \left(v^\star \tilde{r}_0^2 + \|\tilde{\theta}_1\|^2\right)\hat{\eta}(0)^2 + l_1\|\phi_1\|^2 + l_2,\end{aligned} \tag{A.5}$$

$$\begin{aligned}\dot{V}_2 \leq & e^L(\gamma p^\star - v^\star)\tilde{\alpha}^2(L) \\ & - \frac{1}{2}\left(\gamma p^\star - v^\star - \frac{e^L c_3}{2(\gamma p^\star - v^\star)} - e^L c_4\right)\|\tilde{\beta}\|^2 \\ & + \frac{e^L}{2c_4}\|\tilde{\theta}_2\|^2\hat{\eta}(0)^2 + l_3\|\phi_2\|^2 + l_4 + l_5,\end{aligned} \tag{A.6}$$

$$\begin{aligned}\dot{V}_3 \leq & -\frac{v^\star}{2e^L}\hat{\alpha}^2(L) - \frac{1}{2}\left(\frac{v^\star}{e^L} - \frac{c_5}{v^\star} - c_6\right)\|\hat{\alpha}\|^2 \\ & + \left(v^\star \hat{r}_0^2 + \frac{1}{2c_6}\|\hat{\theta}_1\|^2\right)\hat{\eta}(0)^2 + l_6\|\phi_1\|^2 + l_7,\end{aligned} \tag{A.7}$$

$$\begin{aligned}\dot{V}_4 \leq & -\frac{1}{2}\left(\gamma p^\star - v^\star - \frac{e^L c_7}{2(\gamma p^\star - v^\star)} - e^L c_8 - c_9\right)\|\eta\|^2 \\ & - \left(\frac{\gamma p^\star - v^\star}{2} + \frac{e^L K_2^2}{2c_8}\right)\eta^2(0) + l_8\|\phi_2\|^2 + l_9\|\eta\|^2 + l_{10},\end{aligned} \tag{A.8}$$

$$\dot{V}_5 \leq -\frac{\gamma p^\star - v^\star}{2}\|\phi_2\|^2 + e^L(\gamma p^\star - v^\star)\hat{\eta}(0)^2 + l_{11}, \tag{A.9}$$

$$\dot{V}_6 \leq -\frac{v^\star}{2e^L}\|\phi_1\|^2 + v^\star\hat{\eta}(0)^2 + l_{12}, \tag{A.10}$$

where $l_i(t)$ are integrable, nonnegative function of time by applying Lemma 7. And $l_i(t)$ are denoted as

$$l_1 = \partial_t \hat{r}_0^2 + \frac{1}{2v^\star c_1}\|\partial_t\hat{\theta}_1\|^2, \; l_2 = \left(v^\star\tilde{r}_0^2 + \frac{1}{2c_2}\|\tilde{\theta}_1\|^2\right)\tilde{\beta}(0)^2, \tag{A.11}$$

$$l_3 = \frac{e^L\|\partial_t\hat{\theta}_2\|^2}{4c_2(\gamma p^\star - v^\star)}, \; l_4 = \left(e^L\|\tilde{\theta}_2\|^2 - \frac{\gamma p^\star - v^\star}{2}\right)\tilde{\beta}(0)^2, \tag{A.12}$$

$$l_5 = e^L(\gamma p^\star - v^\star)\tilde{r}_1^2 U(t)^2, \; l_6 = \frac{1}{2v^\star c_5}\|\partial_t\hat{\theta}_1\|^2 + \hat{r}_0^2, \tag{A.13}$$

$$l_7 = \left(v^\star\hat{r}_0^2 + \frac{1}{2c_6}\|\hat{\theta}_1\|^2\right)\tilde{\beta}(0)^2, \; l_8 = \frac{e^L(1+K_2^2)\|\partial_t\hat{\theta}_2\|^2}{4c_7(\gamma p^\star - v^\star)}, \tag{A.14}$$

$$l_9 = \frac{2(1+K_2^2)}{c_9}\|\partial_t\hat{\theta}_2\|^2, \; l_{10} = \frac{e^L K_2^2}{2c_8}\tilde{\beta}^2(0), \tag{A.15}$$

$$l_{11} = e^L(\gamma p^\star - v^\star)\tilde{\beta}(0)^2, \; l_{12} = v^\star\tilde{\beta}(0)^2, \tag{A.16}$$

and c_i are positive constants chosen as

$$c_1 = \frac{v^{\star 2}}{2e^L}, \; c_2 = \frac{v^\star}{4e^L}, \; c_3 = \frac{(\gamma p^\star)^2}{e^L}, \tag{A.17}$$

$$c_4 = \frac{(\gamma p^\star - v^\star)}{4e^L}, \; c_5 = \frac{v^{\star 2}}{2e^L}, \; c_6 = \frac{v^\star}{4e^L}, \tag{A.18}$$

$$c_7 = \frac{(\gamma p^\star)^2}{e^L}, \; c_8 = \frac{(\gamma p^\star - v^\star)}{4e^L}, \; c_9 = \frac{(\gamma p^\star - v^\star)}{8}. \tag{A.19}$$

Consider the following Lyapunov function $V = g_1V_1 + V_2 + V_3 + g_2V_4 + V_5 + V_6$, and g_1 and g_2 are positive constants defined as

$$g_1 = 2e^{2L}\frac{\gamma p^\star - v^\star}{v^\star}, \tag{A.20}$$

$$\begin{aligned}g_2 = & \frac{2(\gamma p^\star - v^\star)}{(\gamma p^\star - v^\star)^2 + 4e^{2L}K_2^2}\left(\frac{2e^{2L}(\gamma p^\star - v^\star)}{v^\star}\left(v^\star\tilde{r}_0^2 + \|\tilde{\theta}_1\|^2\right)\right. \\ & \left. + \frac{2e^{2L}}{\gamma p^\star - v^\star}\|\tilde{\theta}_2\|^2 + \left(v^\star + \frac{2e^L}{v^\star}\right)\Theta^2 + e^L\gamma p^\star - e^L v^\star + v^\star\right),\end{aligned} \tag{A.21}$$

we have

$$\dot{V} \leq -g_0 V + lV + l, \tag{A.22}$$

where g_0 is a positive constant defined as

$$g_0 = \min\left(\frac{v^\star}{4}, \frac{\gamma p^\star - v^\star}{8}\right), \tag{A.23}$$

and l is the linear combination of l_i and therefore is also integrable, nonnegative function of time. Since $\frac{1}{2e^L}\|\tilde{\alpha}\|^2 \leq V_1 \leq \frac{1}{2}\|\tilde{\alpha}\|^2$, $\frac{1}{2}\|\tilde{\beta}\|^2 \leq V_2 \leq \frac{e^L}{2}\|\tilde{\beta}\|^2$, $\frac{1}{2e^L}\|\hat{\alpha}\|^2 \leq V_3 \leq \frac{1}{2}\|\hat{\alpha}\|^2$, $\frac{1}{2}\|\eta\|^2 \leq V_4 \leq \frac{e^L}{2}\|\eta\|^2$, $\frac{1}{2e^L}\|\phi_1\|^2 \leq V_5 \leq \frac{1}{2}\|\phi_1\|^2$ and $\frac{1}{2}\|\phi_2\|^2 \leq V_6 \leq \frac{e^L}{2}\|\phi_2\|^2$. Then V is bounded and integrable (Lemma D.3. in Smyshlyaev and Krstic (2010)), and the following holds that

$$\|\tilde{\alpha}\|, \|\tilde{\beta}\|, \|\hat{\alpha}\|, \|\eta\|, \|\phi_1\|, \|\phi_2\| \in \mathscr{L}_2 \cap \mathscr{L}_\infty. \tag{A.24}$$

Then with the inverse transformation (222)–(224) from the final target system $(\tilde{\alpha}, \tilde{\beta}, \hat{\alpha}, \hat{\eta}, \phi_1, \phi_2)$ to $(\bar{w}, \bar{v}, \hat{\psi}, \phi_1, \phi_2)$-system, we have

$$\|\bar{w}\|, \|\bar{v}\| \in \mathscr{L}_2 \cap \mathscr{L}_\infty. \tag{A.25}$$

Finally, from the inverse transformation (43)–(44) from $(\bar{w}, \bar{v})$-system to $(\tilde{q}, \tilde{v})$-system, we get

$$\|\tilde{q}\|, \|\tilde{v}\| \in \mathscr{L}_2 \cap \mathscr{L}_\infty. \tag{A.26}$$

A.2. Convergence

The above Lyapunov proof shows that $\dot{V}$ is bounded from above and V is positive and integrable. According to Lemma D.2. in Smyshlyaev and Krstic (2010), we have

$$\|\bar{w}(x,t)\| \to 0, \; \|\bar{v}(x,t)\| \to 0. \tag{A.27}$$

The inverse transformation (43)–(44) from $(\bar{w}, \bar{v})$-system to $(\tilde{q}, \tilde{v})$-system gives that

$$\|\tilde{q}(x,t)\| \to 0, \; \|\tilde{v}(x,t)\| \to 0. \quad \square \tag{A.28}$$

References

Anfinsen, H., & Aamo, O. M. (2018). Adaptive control of linear 2 ×2 hyperbolic systems. *Automatica*, *87*, 69–82.

Anfinsen, H., Diagne, M., Aamo, O. M., & Krstic, M. (2016). An adaptive observer design for $n + 1$ coupled linear hyperbolic PDEs based on swapping. *IEEE Transactions on Automatic Control*, *61*(12), 3979–3990.

Auriol, J., & Meglio, F. Di. (2016). Minimum time control of heterodirectional linear coupled hyperbolic PDEs. *Automatica*, *71*, 300–307.

Aw, A., & Rascle, M. (2000). Resurrection of second order models of traffic flow. *SIAM Journal on Applied Mathematics*, *60*(3), 916–938.
Belletti, F., Huo, M., Litrico, X., & Bayen, A. M. (2015). Prediction of traffic convective instability with spectral analysis of the Aw–Rascle–Zhang model. *Physics Letters A*, *379*(38), 2319–2330.
Cassidy, M. J., & Windover, J. R. (1995). Methodology for assessing dynamics of freeway traffic flow. *Transportation Research Record*,(1484), 73–79.
Coron, J.-M., Vazquez, R., Krstic, M., & Bastin, G. (2013). Local exponential H2 stabilization of a 2×2 quasilinear hyperbolic system using backstepping. *SIAM Journal on Control and Optimization*, *51*, 2005–2035.
D'Abbicco, M., & Reissig, M. (2014). Semilinear structural damped waves. *Mathematical Methods in the Applied Sciences*, *37*(11), 1570–1592.
Daganzo, C. F. (1995). Requiem for second-order fluid approximations of traffic flow. *Transportation Research, Part B (Methodological)*, *29*(4), 277–286.
Deutscher, J. (2017a). Backstepping design of robust state feedback regulators for linear 2×2 Hyperbolic Systems. *IEEE Transactions on Automatic Control*, *62*(10), 5240–5247.
Deutscher, J. (2017b). Finite-time output regulation for linear 2×2 hyperbolic systems using backstepping. *Automatica*, *75*, 54–62.
Deutscher, J. (2017c). Output regulation for general linear hetero-directional hyperbolic systems with spatially-varying coefficients. *Automatica*, *85*, 34–42.
Fan, S., Herty, M., & Seibold, B. (2013). Comparative model accuracy of a data-fitted generalized Aw-Rascle-Zhang model. arXiv preprint arXiv:1310.8219.
Fan, S., Herty, M., & Seibold, B. (2013). Comparative model accuracy of a data-fitted generalized Aw-Rascle-Zhang model. arXiv preprint arXiv:1310.8219.
Flynn, M. R., Kasimov, A. R., Nave, J. C., Rosales, R. R., & Seibold, B. (2009). Self-sustained nonlinear waves in traffic flow. *Physical Review E*, *79*(5), 056113.
Greenshields, B. D., Bibbins, J. R., Channing, W. S., & Miller, H. H. (1935). A study of traffic capacity. In *Highway research board proceedings*: *Vol. 14*.
Hasan, A., Aamo, O. M., & Krstic, M. (2016). Boundary observer design for hyperbolic PDE–ODE cascade systems. *Automatica*, *68*, 75–86.
Hu, L., Meglio, F. Di., Vazquez, R., & Krstic, M. (2016). Control of homodirectional and general heterodirectional linear coupled hyperbolic PDEs. *IEEE Transactions on Automatic Control*, *61*(11), 3301–3314.
Karafyllis, I., Bekiaris-Liberis, N., & Papageorgiou, M. (2017). Analysis and Control of a Non-Standard Hyperbolic PDE Traffic Flow Model. arXiv preprint arXiv:1707.02209.
Lighthill, M. J., & Whitham, G. B. (1955). On kinematic waves. II. A theory of traffic flow on long crowded roads. *Proceedings of the Royal Society of London. Series A, Mathematical and Physical Sciences*, 317–345.
Meglio, F., Argomedo, F. B., Hu, L., & Krstic, M. (2016). *Stabilization of coupled linear heterodirectional hyperbolic PDE–ODE systems*.
Meglio, F. Di., Vazquez, R., & Krstic, M. (2013). Stabilization of a system of $n + 1$ coupled first-order hyperbolic linear PDEs with a single boundary input. *IEEE Transactions on Automatic Control*, *58*(12), 3097–3111.
Payne, H. J. (1971). Models of freeway traffic and control. *Mathematical Models of Public Systems*.
Richards, P. I. (1956). Shock waves on the highway. *Operations Research*, *4*(1), 42–51.
Seibold, B., Flynn, M. R., Kasimov, A. R., & Rosales, R. R. (2012). Constructing set-valued fundamental diagrams from jamiton solutions in second order traffic models. arXiv preprint arXiv:1204.5510.
Smyshlyaev, A., & Krstic, M. (2010). *Adaptive control of parabolic PDEs*. Princeton University Press.
Su, L., Wang, J. M., & Krstic, M. (2017). Boundary feedback stabilization of a class of coupled hyperbolic equations with non-local terms. *IEEE Transactions on Automatic Control*.
Vazquez, R., Krstic, M., & Coron, J. M. (2011). Backstepping boundary stabilization and state estimation of a 2×2 linear hyperbolic system. In *Decision and control and European control conference (CDC-ECC) 2011 50th IEEE conference on* (pp. 4937–4942). IEEE.
Whitham, G. B. (2011). *Linear and nonlinear waves (Vol. 42)*. John Wiley & Sons.
Yu, H., Vazquez, R., & Krstic, M. (2017). Adaptive output feedback for hyperbolic PDE pairs with non-local coupling. In *American control conference (ACC) 2017* (pp. 487–492). IEEE.
Zhang, H. M. (2002). A non-equilibrium traffic model devoid of gas-like behavior. *Transportation Research, Part B (Methodological)*, *36*(3), 275–290.
Zhang, L., & Prieur, C. (2017). Necessary and sufficient conditions on the exponential stability of positive hyperbolic systems. *IEEE Transactions on Automatic Control*.

Huan Yu received the B.S.degree in Aerospace Engineering from Northwestern Polytechnical University, China and the M.S. degree in Mechanical and Aerospace Engineering from University of California, San Diego, USA. She is currently pursuing the Ph.D. degree in Mechanical and Aerospace Engineering at University of California, San Diego, USA. Her research focuses on the control and estimation of distributed parameter system, and the main applications include transportation system and structural system.

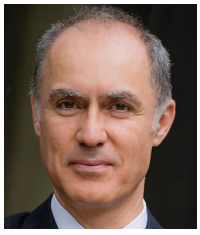

Miroslav Krstic is Distinguished Professor of Mechanical and Aerospace Engineering, holds the Alspach endowed chair, and is the founding director of the Cymer Center for Control Systems and Dynamics at UC San Diego. He also serves as Senior Associate Vice Chancellor for Research at UCSD. As a graduate student, Krstic won the UC Santa Barbara best dissertation award and student best paper awards at CDC and ACC. Krstic has been elected Fellow of seven scientific societies – IEEE, IFAC, ASME, SIAM, AAAS, IET (UK), and AIAA (Assoc. Fellow) – and as a foreign member of the Academy of Engineering of Serbia. He has received the ASME Oldenburger Medal, Nyquist Lecture Prize, PaynterOutstanding Investigator Award, Ragazzini Education Award, Chestnut textbook prize, the PECASE, NSF Career, and ONR Young Investigator awards, the Axelby and Schuck paper prizes, and the first UCSD Research Award given to an engineer. Krstic has also been awarded the Springer Visiting Professorship at UC Berkeley, the Distinguished Visiting Fellowship of the Royal Academy of Engineering, and the Invitation Fellowship of the Japan Society for the Promotion of Science. He serves as Senior Editor in IEEE Transactions on Automatic Control and Automatica, as editor of two Springer book series, and has served as Vice President for Technical Activities of the IEEE Control Systems Society and as chair of the IEEE CSS Fellow Committee. Krstic has coauthored thirteen books on adaptive, nonlinear, and stochastic control, extremum seeking, control of PDE systems including turbulent flows, and control of delay systems.